2023

Audible and Subaudible Components of the First and Second Heart Sounds Using Phonocardiography and Seismocardiography

Daniella King
University of Central Florida

AUDIBLE AND SUBAUDIBLE COMPONENTS OF THE FIRST AND SECOND HEART SOUNDS USING PHONOCARDIOGRAPHY AND SEISMOCARDIOGRAPHY

by

DANIELLA KING

A thesis submitted in partial fulfillment of the requirements
for the Honors Undergraduate Thesis Program
in the Department of Mechanical and Aerospace Engineering
in the Burnett Honors College
at the University of Central Florida
Orlando, Florida

Spring Term, 2023

Thesis Chair: Hansen A. Mansy, Ph.D.

ABSTRACT

Cardiovascular disease continues to be a leading cause of death in the United States, and a source of financial strain on the healthcare system. This prompts the need for new methods of low-cost, noninvasive technologies for cardiac monitoring to improve patient health and reduce healthcare costs. While the first and second heart sounds are common references that are listened to during auscultation of heart, seismocardiography (SCG) is a technology that detects chest sound vibrations with an accelerometer and may offer more information beyond the audible heart sounds. There is currently limited information regarding both the relationship between audible heart sounds and SCG, as well as the low-frequency (<20 Hz) characteristics of heart sounds. The intent of this thesis is to investigate the relationship between audible heart sounds and SCG, with the goal of understanding the clinical utility of SCG. This was done using both audible and subaudible frequencies. Comparisons indicate the SCG signal carries a greater amount of low-frequency content than audible heart sounds, which warrants further study to determine how SCG can be best harnessed for cardiac monitoring.

ACKNOWLEGDMENTS

Words cannot express my gratitude to my thesis chair, Dr. Hansen Mansy. Several years ago, when I joined the Biomedical Acoustics Research Lab, he introduced me to the foundations of research and fostered a passion for not only this thesis topic, but the research process as a whole. Throughout our time working together, he has been instrumental in providing thoughtful guidance as a mentor. His patience, vast knowledge, and passion are only a few of the qualities that deserve a deep appreciation.

I would like to thank Dr. Richard Sandler, another member of my thesis committee. He kindly provided time amid his busy schedule and his feedback on numerous drafts, presentations, and ideas. I am inspired by his contagious excitement to teach others.

I am tremendously grateful to be part of an excellent team, including Anna Voyatzoglou, Rajkumar Dhar, and Brianna Dinh. Raj made the engineering aspect of this topic understandable and possible, which I could not have done this process without. Anna and Brianna have both been a pleasure to work alongside, constantly putting forth their best efforts and collaborative spirits.

Lastly, I would like to thank my father for his unconditional daily support. His encouragement is integral to all my achievements, and this thesis is no exception.

TABLE OF CONTENTS

LIST OF FIGURES

LIST OF TABLES

CHAPTER 1: INTRODUCTION AND MOTIVATION

Cardiovascular disease (CVD) is one of the leading causes of death worldwide [1] and cost the United States economy approximately 378 billion dollars between 2017 and 2018 [2]. The Centers for Disease Control and Prevention (CDC) recently reported that in only one year, CVD caused approximately 697,000 deaths and on average resulted in one death every 34 seconds [3]. This drives the need for an improved understanding of human cardiac conditions, which may lead to enhanced cardiac diagnostic and monitoring techniques. Low-cost monitoring methods can lead to significant savings for the healthcare system, where costs continue to rise.

One of the current, standard ways to evaluate cardiac status is through electrocardiography (ECG), which monitors the electrical activity during the cardiac cycle. Another standard way of evaluating cardiac status is through auscultation, or listening to heart sounds, typically through a manual or electronic stethoscope. The signal produced by a stethoscope in this way is referred to as phonocardiography (PCG), which detects sounds produced by the heart. While some PCG sensors are well-manufactured and may be able to detect low frequencies adequately, they are generally regarded and intended for audible events.

Seismocardiography (SCG) is another non-invasive technique that may be used to evaluate cardiac status and is measured using an accelerometer. Unlike ECG, which focuses on the electrical aspect, SCG signals provide information from the chest surface about the heart mechanics via the vibrations that are produced by the mechanical activity. Simultaneous recording of ECG can provide a reliable tool to track cardiac cycle stages and align with SCG.

Some cardiac pathologies, such as the diastolic aspect of mitral stenosis, mainly have low frequency (<100 Hz) sound content [4]. This can be difficult to hear with the human ear such as when utilizing a PCG signal via a stethoscope. These instances where low frequencies predominate are an opportunity to harness another technology or enhance current technology for improved ease of detection. Further, there may be other clinically useful information provided by SCG that is simply unknown because it has not been thoroughly investigated. While PCG and SCG are both potential low-cost non-invasive cardiac monitoring techniques, the relationship between audible heart sounds (detected by a PCG sensor) and SCG is not yet well understood. SCG cannot be utilized to its full potential without the understanding of what information it provides and how this relates to audible heart sounds. This gap in knowledge is one of the areas that this thesis aims to address. This will be done by comparing multiple frequency bands, both within and outside, of the typical human hearing range. This data will be investigated to elucidate what missing information may be gathered in the sub-audible range from both a PCG and SCG perspective.

CHAPTER 2: LITERATURE REVIEW

2.1 Cardiac Anatomy and Physiology

The human heart serves to supply the body with oxygenated blood. It allows this circulatory system to function by first collecting de-oxygenated blood, transporting this blood to the lungs where it becomes oxygenated, then pumping the newly oxygenated blood to the tissues of the body. It consists of four chambers to accomplish this (see Figure 1). The right side of the heart has two chambers: the right atrium on the superior aspect and the right ventricle on the inferior aspect. These two chambers are separated by a valve called the tricuspid valve. The right side is supplied by large veins called the superior and inferior vena cave, which contain deoxygenated blood collected from the body. Deoxygenated blood exits from the heart through the pulmonary artery. The pulmonary valve is located between the right ventricle and the pulmonary artery. The left side is supplied by the pulmonary veins, which contain oxygenated blood from the lungs that will be distributed to the body. Oxygenated blood exits the left side of the heart via the aorta, and the aortic valve is located between the left ventricle and aorta. The left side has a left atrium and left ventricle, separated by the bicuspid, or mitral, valve. Separating the left and right sides of the heart is a "wall" of muscle and tissue called the septum. [5]

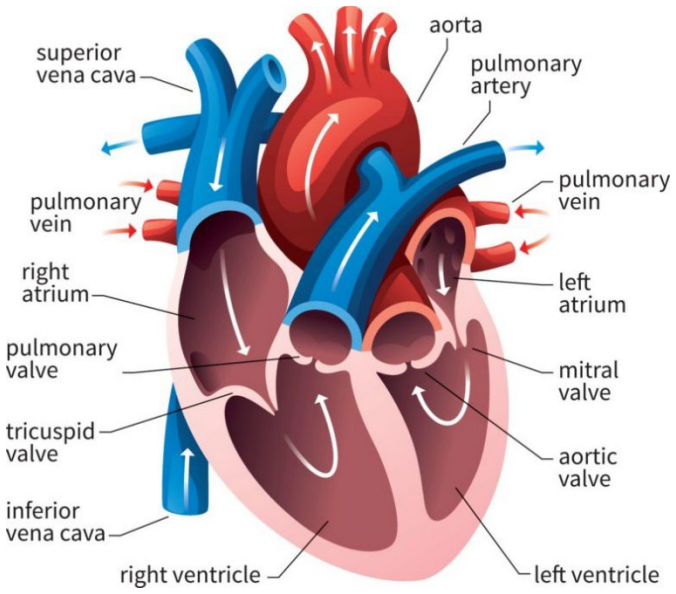

Figure 1: An illustration of the main heart structures and white arrows representing the direction of blood flow [6].

The terms systole and diastole are used to describe the two states of the cardiac cycle. Systole refers to the contraction of the bottom chambers, or the right and left ventricles. The tricuspid and mitral valves remain closed at this time to prevent backflow into the top chambers. Diastole refers to the contraction of the top chambers and the relaxation of the bottom chambers. This allows blood to fill the ventricles while the pulmonary and aortic valves are closed [7].

The heart muscle contractions are induced via the heart's electrical conduction system. This system originates at the sinoatrial (SA) node, also called the pacemaker of the heart. It is located in the upper right atrium and produces a signal that travels inferiorly throughout the heart. The electrical signal takes a path from the SA node to the AV node, down the Bundle of His (which consists of the left and right bundle branches), and disperses through the Purkinje fibers [8]. Figure 2 illustrates this path. This conduction is regulated by ion gradient changes, particularly regarding calcium, sodium, potassium, and magnesium (Ca^{2+}, Na^{+}, K^{+}, and Mg^{2+}, respectively) [9-10].

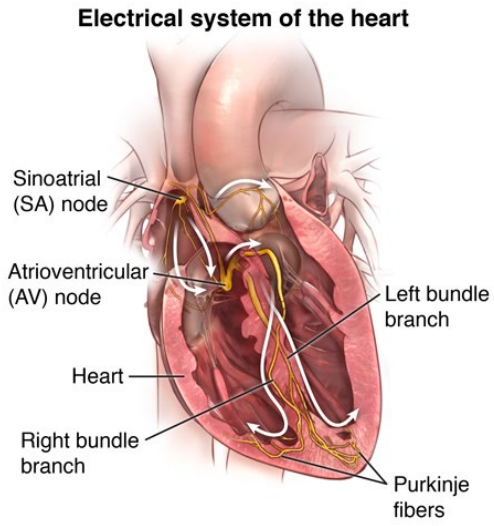

Figure 2: The electrical system of the heart with key landmarks notated and direction of electrical activity [11].

One widely used non-invasive method to gain insight into cardiac function is through auscultation. When listening to sounds produced during the cardiac cycle, there are often two main sounds that are referred to as the first and second heart sounds (S1 and S2). The literature generally concludes that these are the result of valve closures [12]. Although there are also third (S3) and fourth (S4) heart sounds, this study will mainly focus on S1 and S2 as they are the most predominant within the signal and more understood. S1 is believed to be generated by tricuspid and mitral valve closures, while S2 is believed to be generated by aortic and pulmonic valves closures [13].

There are also particular locations at which these sounds are best heard. S1 is best heard at the apex of the heart, which is its inferior aspect. S2, however, is best heard at the base, or the superior aspect, of the heart. Variations in S1 and S2 sounds may be of clinical and diagnostic relevance as they can indicate valve or structural disorders [12].

2.2 Phonocardiography

Phonocardiography (PCG) is a non-invasive method to evaluate some aspects of cardiac status and auscultating a patient is often a key aspect of a physical exam. A phonocardiogram is the recording of sounds or murmurs mechanically produced by the heart. It is shown as a waveform that is the visual representation of the heart sound signal. These acoustic signals are typically obtained using a microphone integrated with a stethoscope [13]. While it is mainly used to visualize audible heart sounds, some PCG sensors may also detect subaudible sounds. PCG as a technology originated between the 1930s-40s although became standardized in approximately 1950 [14]. In a PCG signal, as shown in Figure 3, the S1 and S2 events are fairly distinct within each heartbeat.

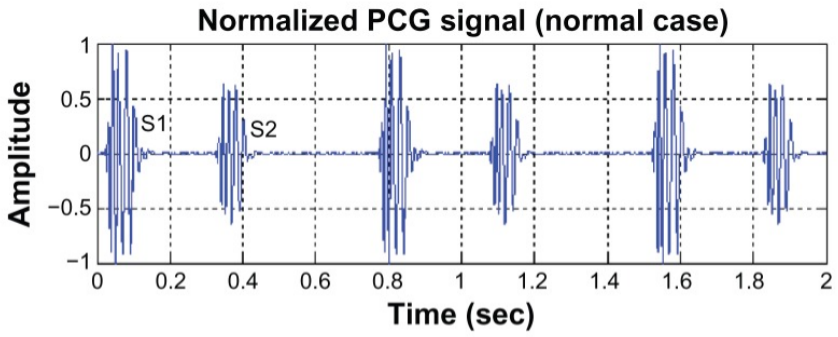

Figure 3: A normal PCG signal with labelled S1 and S2 events [15].

These mechanically (as opposed to electrically) produced signals are generally believed to be the result of valve closures and the corresponding blood flow [16]. The waveform, frequency and amplitude are all factors that may be investigated and may have clinical significance. This electronic approach provides an advantage over listening with the human ear as the former provides an objective recording of sounds.

Figure 4 provides a visual representation of the main auscultation locations. The most routine four cardiac auscultation locations are the aortic, tricuspid, pulmonic, and mitral areas. A fifth traditional auscultation location is Erb's point. The aortic point is on the patient's right side at approximately the second intercostal space (ICS). The pulmonic area is reflected across the sternum from the aortic area. The tricuspid area is at the fourth ICS, directly below the pulmonic area at the left sternal border. The mitral area is further inferior and is located the midclavicular line and the left fifth ICS [17].

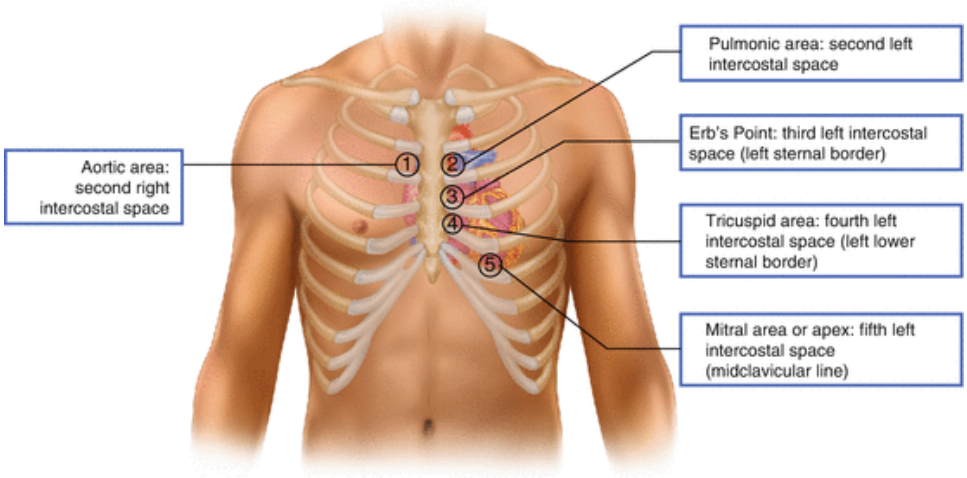

Figure 4: The typical auscultation locations on the chest surface [17].

2.3 Electrocardiography

Electrocardiography (ECG) is a widely used, reliable non-invasive technology that acquires a signal that represents the heart's electrical activity.

The "Father of Modern Electrocardiography," Willem Einthoven, received this title for his early measurements of cardiac electrical activity using a String Galvanometer in 1902 [14].

Since then, electrocardiography has developed into a pivotal part of evaluating cardiac status. It is often offered through a portable device that uses electrodes that are placed on the surface of the body. A "12-lead ECG," which involves 10 electrodes, is commonly used [18]. However, variations of the number and locations of electrodes are also implemented to understand conduction through the heart. One such example includes "Einthoven's Triangle," named after Willem Einthoven. In this setup, a total of three electrodes are placed, with one on each arm and another on the left leg [19]. Figure 5 indicates this arrangement with the abbreviations "RA" (right arm), "LA" (left arm), and "LL" (left leg). Given the electrical basis of cardiac conduction, the measurement for ECG is reported in voltage.

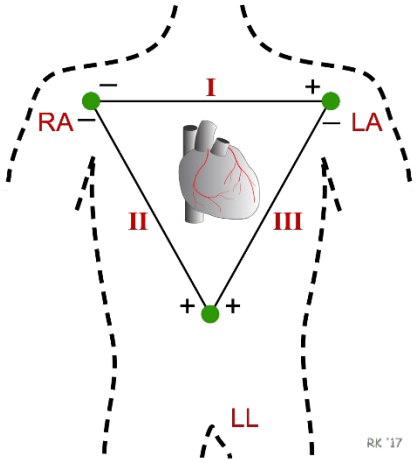

Figure 5: Einthoven's Triangle [19].

A typical ECG signal for a single heartbeat has several components including a P wave, QRS complex, and T wave. The P wave represents atrial depolarization. The QRS complex consists of the Q, R, and S waves. The Q wave is a downward deflection that represents the depolarization of the septum in between the ventricles. The R wave signifies depolarization of the majority of the ventricles. The S wave signifies the depolarization of the remaining parts of

the ventricles. The T wave represents repolarization of the ventricles. While the QRS complex occurs, the atria repolarize although this is masked by the strong QRS activity [20].

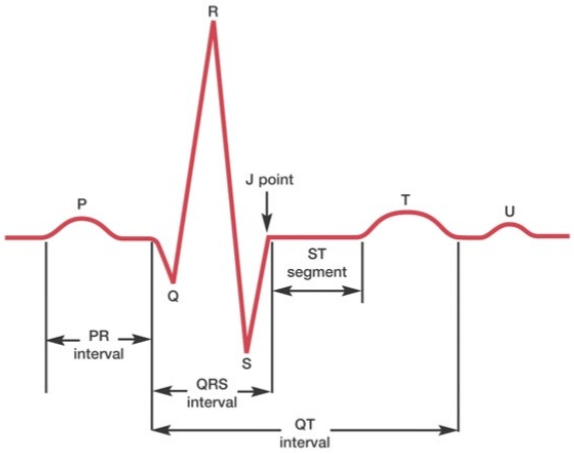

Figure 6: A normal ECG signal [20].

Different aspects of the ECG can be analyzed to determine normal or abnormal function. Some of these characteristics include the rate of electrical conduction (therefore the heartbeat), the rhythm, and waveform morphology irregularities [20]. Some conditions that can be discerned through an EKG include abnormal rhythm, coronary artery disease, or valve diseases [21]. For these reasons, as well as reliability, low cost, and convenience, ECG is often considered a "gold standard" in cardiac monitoring and diagnostics.

2.4 Seismocardiography

Seismocardiography is another non-invasive technology although it uses an accelerometer to record cardiac vibrations caused by mechanical movement of the heart [22]. The best use of SCG is in a relatively low-frequency range, which is described as <50 Hz in [23]. It originated as a technology in the 1960s although made its appearance in clinical medicine in

the 1980s [24]. It has not gained traction as a clinical instrument due to the overpowering advancements of other technologies such as ECG [25]. However, if SCG is better understood, it may prove to be a useful monitoring and diagnostic tool.

A common location to place the sensor is near the sternum, particularly the lower left sternal border [26]. The morphology of the waveform is typically more complex and variable than ECG or PCG signals. However, SCG can be grouped into clusters that bear similarities within each cluster. Studies suggested that respiration, whether related to airflow direction or lung volume changes, may be one of the factors that causes variabilities in SCG events and can also be a method for grouping similar events [26]. Additionally, SCG sensors are sensitive to their placement location, and it is thus important to ensure correct placement when using accelerometers for SCG measurements.

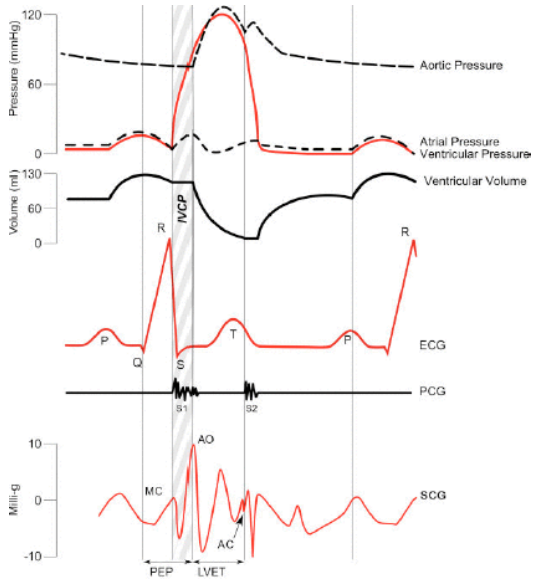

Figure 7: Various signals in a healthy subject. The bottom horizontal line (in red) represents a normal SCG signal. Comparison can be made against the two red horizontal lines above this, representing PCG and ECG [24].

CHAPTER 3:

OVERVIEW OF DATA ACQUISITION AND METHODOLOGY

3.1 Overview and Objectives

There are two overall goals of this study, each with subgoals:

1) Confirm spatial distribution results of the measured audible heart sounds (as measured by S1/S2 ratio with PCG sensors) and compare these results with the literature.

This will be done to provide confidence in the study methods and instruments used. Additionally, the results of PCG sensor spatial distribution, as measured by S1/S2 ratio, will be reported in the sub-audible and full frequency range. See Table 1 for the parameters of each range.

Table 1: Criteria for the three frequency ranges.

Full range	0-100 Hz
Sub-audible range	0-20 Hz
Audible range	20-100 Hz

2) Establish a relationship between audible heart sounds (via PCG sensors) and SCG.

This will be done to fill the gap in current knowledge between their relationship. It will be accomplished using accelerometers to measure SCG at three chest surface locations. These SCG signals will be compared with signals from PCG sensors recorded on the same subject.

3.2 Research Questions and Hypotheses

In accordance with section 3.1, the research questions and corresponding hypotheses are:

- Questions pertaining to audible heart sounds: Is S1 louder at the inferior location? Is the S1/S2 ratio greater at the inferior location? (As measured with PCG sensors.)
    - Hypotheses: S1 is generated by the closure of the atrioventricular (mitral and tricuspid) valves while S2 is generated by closure of semilunar (aortic and pulmonary) valves. If this is true, an extension of this hypothesis is that S1, relative to S2, is expected to be louder in an inferior location. Similarly, the S1/S2 ratio is expected to be greater at an inferior location.
    - Approaches: S1 at one location may be compared to S1 at a different location. Also, S1 may be compared to S2 within one sensor (therefore at one location).
- Questions pertaining to the relationship between audible heart sounds and SCG: How does signal from the accelerometer, gathering SCG signal, compare to stethoscope, gathering PCG signal? Is the PCG signal a representation of the audible range of SCG?
    - Hypotheses: PCG signal (as measured with electronic stethoscope) represents the audible range of SCG (as measured with accelerometer).
    - Approaches: Investigate the audible component of SCG to compare its similarity to the audible component of PCG. Comparison may be accomplished through the S1/S2 ratio and SCG1/SCG2 ratio, amplitude, and waveform comparison. Additionally, this may include auditory comparison by listening to PCG sensor and SCG sensor recordings of the same subject and comparable locations.

3.3 Procedures

3.3.1 Preliminary Testing – Waveform and Signal to Noise Ratio

Prior to collecting the data used on human subjects, extensive and thorough preliminary studies were conducted on the sensors to develop a solid foundation and ensure confidence in later results. The main procedures and conclusions will be discussed here to provide a groundwork for the main results discussed in this paper, although the full report may be found in [27].

One of the first considerations was that of microphone choice, which would be later paired with stethoscopes. Two microphones were mainly considered: lavalier microphones and PCB Piezotronics. When both microphones were used to detect a pre-recorded PCG signal (which was played back at the surface of a special "phantom"), the PCB microphone produced an amplitude approximately three times that of the lavalier although the morphology of signals produced by both microphones was quite similar. Ultimately, the lavalier microphone style was chosen because of their ideal lightweight characteristic, similarity in morphology to the well-respected PCB, and plentiful stock available. The several lavaliers that were chosen were compared for similar Signal-to-Noise (SNR) ratio and produced satisfactorily similar results.

Figure 8: Lavalier microphone (left) and PCB microphone (right).

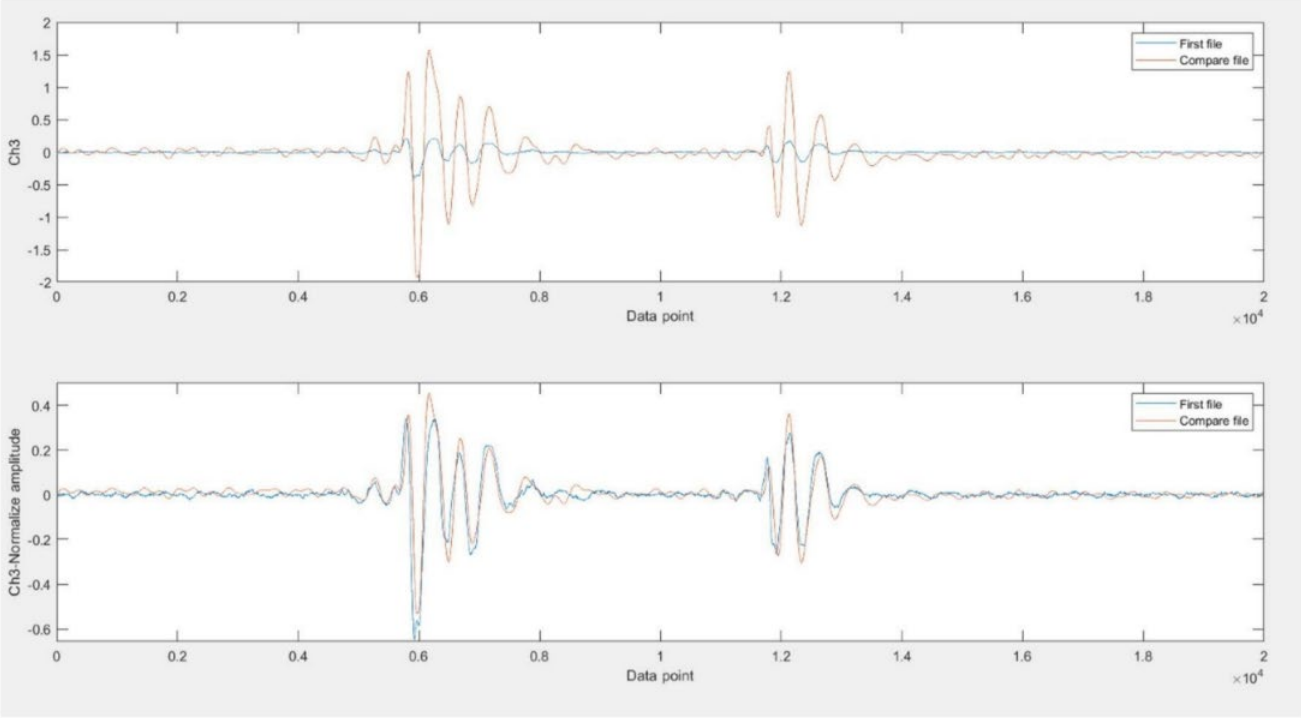

Figure 9: The top graph is the non-normalized comparison between the PCB microphone (orange) and the Lavalier microphone (blue) when detecting a pre-recorded PCG signal. The bottom graph is the normalized comparison to better appreciate the similarity in morphology.

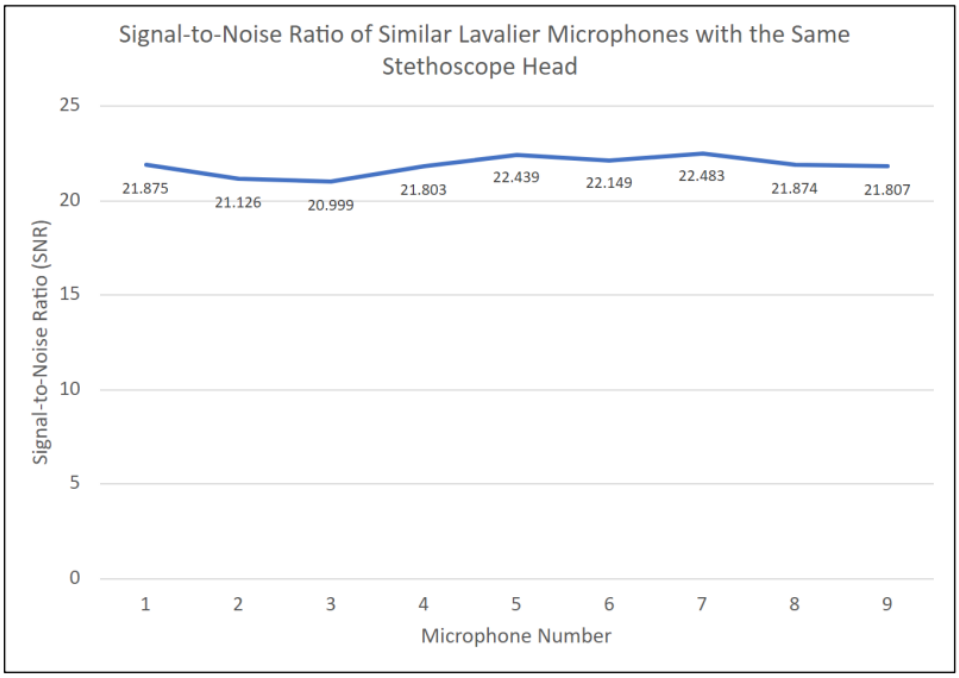

Figure 10: This graph indicates the SNR for 9 tested lavalier microphones, of which the most similar ones were chosen from.

In regard to stethoscope chest piece choice, nine stethoscopes were gathered and initially considered (see Figure 11).

Figure 11: Nine stethoscopes that were originally considered numbered 1-9, from left to right.

Stethoscope 8, manufactured by "Zulco" and purchased from Amazon, was quickly ruled out. This is because it was determined by the researchers to leak air from the bell-tubing connection based on the waveform morphology and amplitude. Following this, six different stethoscopes (1, 3-7) were tested against a 3M Littman stethoscope chestpiece (stethoscope 2).

The Littman was placed in the position of comparison for each situation for the purpose of serving as a “gold standard” due to its reputable manufacturing and quality. The waveform comparison is found in Figure 12 and the same microphone was used in each case for consistency. From this, Stethoscope 1 (Labtron) was eliminated from progressing to selection due to the distorted waveform, ringing, and large, bulky size that would not fare well to balance on the chest surface.

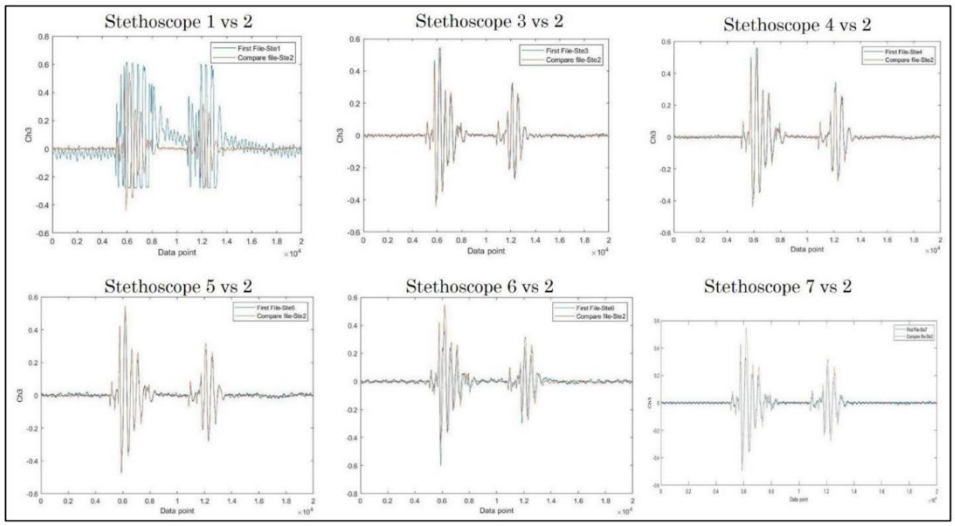

Figure 12: Waveform comparisons of stethoscopes 1,3-7 against Stethoscope 2, the 3M Littmann. “Stethoscope 1 for Labtron, Stethoscope 3 for Bio-Dynamics, Stethoscope 4 for ADC Proscope, Stethoscope 5 for 3D printed, Stethoscope 6 for 3D printed, and Stethoscope 7 for unknown model.” [27]

Aside from investigating the morphology of each of these stethoscopes, the SNR of the remaining stethoscopes was also considered as an important factor and tested. This was accomplished by comparing PCG signal vs the no input signal, and white noise vs no the input signal. The results are found in Figure 13, and it was determined that this did not immediately rule out any stethoscope heads because their SNR range was similar and high enough to be considered satisfactory.

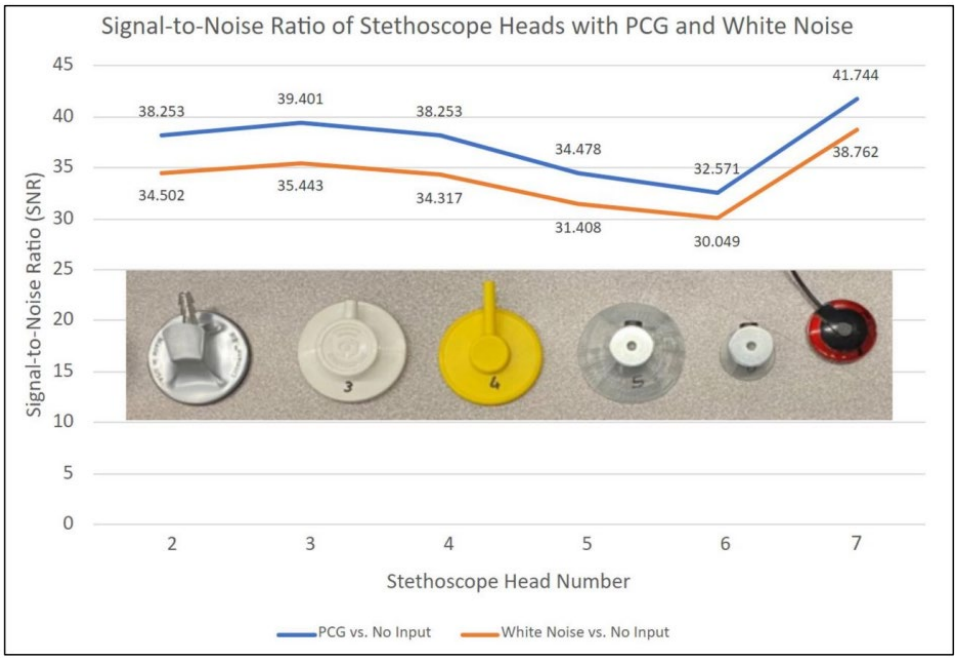

Figure 13: SNR for Stethoscopes 2-7.

Following the testing done of stethoscopes 2-7, the PARAMED stethoscope (pictured rightmost in Figure 11) was also tested and yielded similar results. Because of its small size, light weight, readily available stock, and similar results it was selected to be the stethoscope of choice for the study.

This preliminary study allowed the researchers to deliberately choose the equipment, thereby building a strong foundation for future data collection, and an understanding of the frequency response for the chosen equipment.

3.3.2 Stage 1:

Data Acquisition by Recording ECG, PCG and SCG Data on Human Subjects

This stage was completed through previous studies completed at the lab and may be referenced in [27] which contains thorough documentation. A summary of the relevant protocol from the paper has been provided below:

- Recruited college-aged, female and male volunteer subjects that do not have a known history of cardiovascular disease.
- Subject arrived at testing site, briefed on procedure, and completed data collection form.
- Sensor locations on the body were cleansed and prepared. ECG, PCG, and SCG sensors were placed in Arrangement A (see Figures 12 and 13) on the subject. Galvanic skin response electrodes were included for monitoring of subject's breathing patterns.
- Subject rested supine at a 45-degree angle on examination table for three minutes.
- The first recording was gathered and saved using iWorx Labscribe:
    - 1. Three minutes of normal breathing.
    - 2. Two minutes of slow, deep breathing.
    - 3. One minute of normal breathing.
    - 4. Three breath holds, duration dictated by the subject [27].
- Arrangement A sensors were removed as needed to switch to Arrangement B configuration. Sensors specific to Arrangement B (see Figure 15) were placed.
- The second recording (Arrangement B) was gathered and saved using iWorx Labscribe. With the exception of sensor location and type, the procedure was carried out the same as Arrangement A.

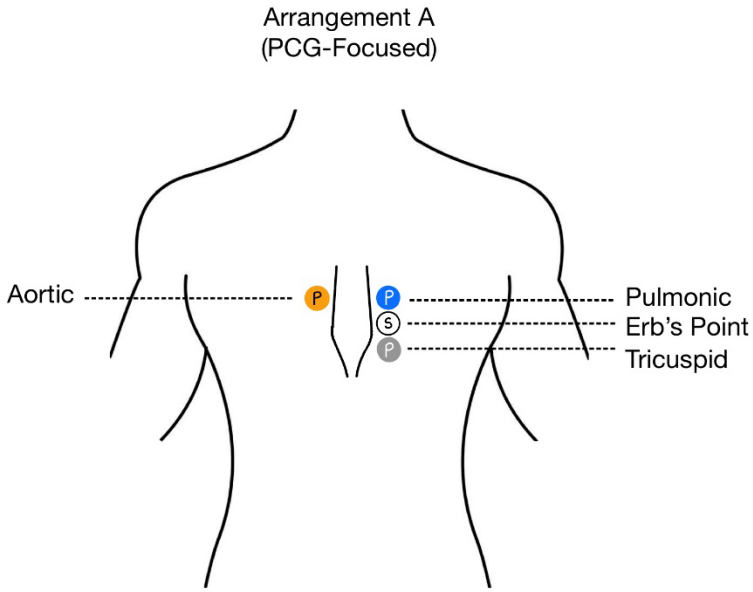

Figure 14: Arrangement A, which is a PCG-focused configuration. 3 PCG sensors (at aortic, pulmonic, and tricuspid locations) and 1 SCG sensor (at Erb's point location) are used.

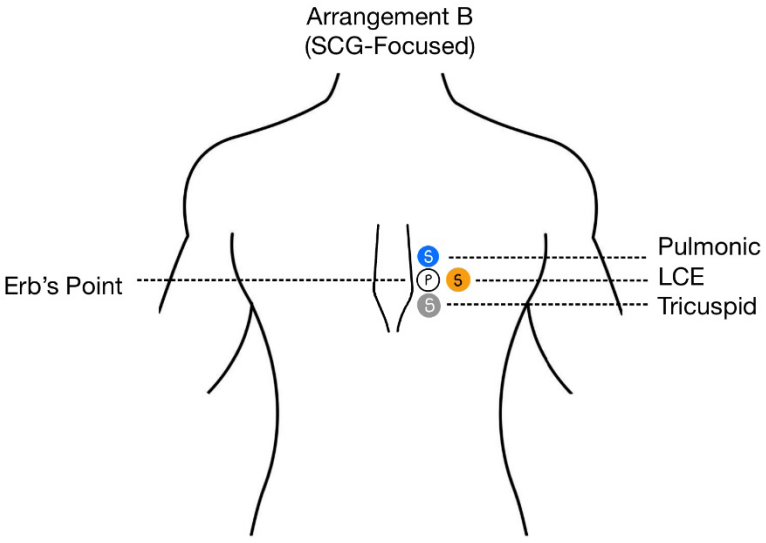

Figure 15: Arrangement B, which is a SCG-focused configuration. 3 SCG sensors (at pulmonic, LCE, and tricuspid locations) and 1 PCG sensor (at Erb's point location) are used.

Figures 14 and 15 provide a useful visual description of sensor locations from this point forward. Sensors may be referred to by the name of their location (ex: tricuspid sensor). Additionally, LCE is the abbreviation for the sensor that is “laterally contiguous to Erb’s.”

3.3.3 Stage 2: Analysis of PCG Data

The procedure for this stage is as follows:

- Signals collected from Arrangement A are processed using MATLAB.
- Pan-Tompkins algorithm is used to detect ECG R-waves. PCG signals are segmented using the corresponding ECG R-waves.
- S1 and S2 are detected as the points of maximum amplitude at certain time windows of each PCG event.
- In situations where the data was particularly noisy and unreliable, one or several beats are manually removed from the computer calculations as needed.
- The average ratio of S1 to S2 amplitudes (S1/S2 ratio) over all the PCG segments is calculated at each sensor location for each subject.
- The analysis is performed for the full range, audible, and sub-audible frequency bands of the PCG signal.
- The resulting S1/S2 ratio and standard deviation is recorded in an Excel file.

3.3.4 Stage 3: Analysis of SCG Data

SCG sensor data was analyzed through MATLAB using the same format that the PCG data was analyzed in Stage 2 to compare the SCG1/SCG2 ratio at particular chest locations and frequency bands between the two sensors. Plots were generated using Excel based on data collected with MATLAB.

The quantification method for audible heart sounds and SCG comparison was accomplished using an "S1/S2 ratio" for PCG signal and "SCG1/SCG2 ratio" for SCG signal. This refers to the ratio of S1 amplitude to S2 amplitude at a particular location. This will likely be affected by both chest location as well as the frequency band that is used. For a richer comparison, other methods may be used to determine differences, and this is discussed in the Future Work section.

3.3.5 Stage 4: Analyze and Compare Trends in Subaudible, Audible and Full Range for Both PCG and SCG

The procedure to compare the PCG and SCG signals, in three frequency ranges, involved generating plots using Excel based off data collected in MATLAB. The data used includes the three instances in which the location of sensor was same for PCG and SCG, although these were not recorded at the same time. The mean S1/S2 ratio was mainly used as the variable to determine similarities or differences. T-tests were applied to determine significance in terms of p-value and provide quantifiable data comparisons.

3.4 Materials

The materials for data acquisition are as follows:

- Three stethoscope heads: Single Head Stethoscope, PARAMED
    - Paired to three microphones lavalier purchased through Amazon (specifications unavailable)
- Data acquisition module to connect to sensors: Model TA-220, iWorx, Dover, NH
- Recording module for ECG and GSR: iWire-B3G, iWorx, Dover, NH
- Software (Including LabScribe, iWorx, TA-220, Dover, NH) on laptop computer (Model Latitude 3590, Dell, 2018)
- Amplifier: PCB Piezotronics, Model 482C Series, Depew, NY
    - For amplification of SCG signal.
- Subjects to perform study on.

After preliminary testing, sensors and attachment methods were chosen:

- 5 Reusable Button EEG Electrodes: Model C-ISO-GC5, iWorx, Dover, NH
- 3 ECG electrodes Model FS-TB1-5, Skintact, Innsbruck, Austria
- 2 Galvanic Skin Response Sensors: Model C-ISO-GSR, iWorx, Dover, NH
- Double-sided medical tape: Double Coated Tape 444, 3M,

Materials of Data Analysis and Miscellaneous:

- Software: MATLAB (R2022a, MathWorks, 2022), Microsoft Excel (Microsoft, 2021)
- Standard examination table
- Alcohol wipes

- Quiet location to perform experiment

3.5 Participants

Data from 31 total subjects was recorded. Of these 31, 23 are female and the remaining 8 are male. The ages range from 18 – 31 years. 24 subjects were ultimately analyzed, composed of 17 females and 7 males with a mean age of 21.54 and standard deviation of 2.63 years.

Of the 7 remaining subjects that were not analyzed, explanations are offered in the remainder of the paragraph. One subject only had an Arrangement A recording saved and it is possible that the Arrangement B recording was not saved at the time of the study, unbeknownst to the researchers. Another subject had a disruption of Arrangement B recording at approximately 55 seconds and in Arrangement A at approximately 1 minute and 21 seconds. Another subject had a disruption of Arrangement A recording near 1 minute and 20 seconds. Presently, the reason for the disruptions remains unclear. It is likely that the subject shifted positions at those times positions or created a disturbance such as by coughing or sneezing. The four remaining subjects' recordings were unable to be found in the file directory where other recordings were stored. When possible, further investigation is encouraged.

Regrettably, the data collection form that was completed by subjections prior to undergoing the study (Figure 16) was not as clarificatory as possible. The question, "Do you have a history of cardiovascular health problems, personally or in your family," was optional. Furthermore, it did not require specification of what the potential condition is, and if it is of the subject or the subject's family. Documentation of positive or blank responses to the question are as follows:

- Subject 2: Yes, history of cardiovascular health problems in family
- Subject 4: Yes, history of cardiovascular health problems in family
- Subject 7: Yes, history of cardiovascular health problems in family
- Subject 8: Yes, history of cardiovascular health problems in family
- Subject 9: Yes, history of cardiovascular health problems in family
- Subject 10: Yes, history of cardiovascular health problems in family
- Subject 11: Yes, history of cardiovascular health problems in family
- Subject 12: “Unknown”
- Subject 13: Yes, history of cardiovascular health problems in family
- Subject 14: Yes, (unspecified whether in subject or their family)
- Subject 16: Yes, arrythmia (unspecified whether in subject or their family)
- Subject 19: Yes, history of cardiovascular health problems in family
- Subject 22: Did not answer this question
- Subject 23: Yes, history of cardiovascular health problems in family

SCG/PCG Study – Data Collection Form

Date. _____

E-mail address. _____

Name and initials. _____

Age. _____

Biological sex. _____

Height. _____

Weight. _____

Have you had caffeine recently?
If so, when? _____

When did you last eat? _____

The following questions are optional; please answer only if you are comfortable doing so.

How many hours a week do you exercise on average? _____

Do you have a history of cardiovascular health problems, personally or in your family? _____

Are you currently taking medications that might affect blood circulation or cardiac activity?
If so, what? _____

Have you tested positive for COVID-19 at any point? If so, when? _____

If you menstruate, when was your last period? _____

Figure 16: The Data Collection Form filled out by subjects immediately prior to testing.

CHAPTER 4: RESULTS AND ANALYSIS

The results are divided into three logical sections for comparison: Phonocardiography Data (section 4.1), Seismocardiography Data (4.2), and Comparison of Phonocardiography and Seismocardiography Data (section 4.3). The first section, 4.1, reflects data that was collected in Arrangement A, the PCG-heavy arrangement (Figure 14). The second section, 4.2, reflects data from Arrangement B, the SCG-heavy arrangement (Figure 15). The third section compares data from 4.1 and 4.2 at three instances of identical sensor locations. At the end of each section, there will are tables that summarize quantitative factors pointed out in individual cases.

4.1 Phonocardiography Data

Three sensor locations were studied for this phonocardiography-only section: pulmonary, tricuspid, and aortic. The plots on the left side of the page indicate the mean S1/S2 ratio for two locations, for each subject. The plots on the right side of the page indicate the *difference* in mean S1/S2 ratio of two locations for each subject.

Additionally, to present the results in the for three different frequency ranges of interest (see Table 1), a total of six plots were generated for each two locations compared against each other. T-tests were calculated to determine p-value, which indicates the significance in the difference of mean S1/S2 ratio between locations. The number of subjects (out of the 24 total) that had a "difference of mean S1/S2 ratio" > 0 was also included for analysis as another quantitative measurement.

A thorough explanation will be provided for the figure below (Figure 17) and the reader may apply this logic to the following figures in Section 4.1.1 and 4.1.2. If there are noteworthy trends or analysis unique to a particular pair of graphs, that information will be found below the graphs it pertains to.

4.1.1 PCG - Tricuspid vs Pulmonary for All Three Frequency Ranges

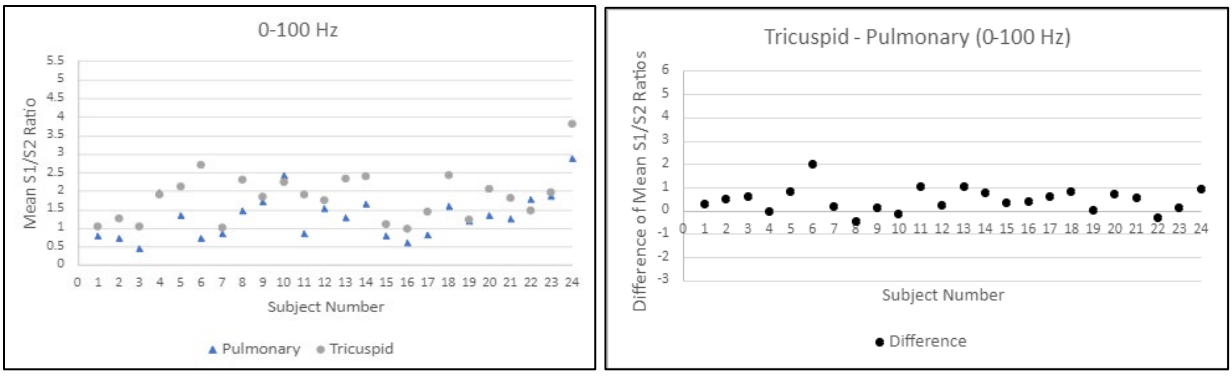

Figure 17: Mean S1/S2 ratio (left) and difference of mean S1/S2 ratio (right) in 0-100 Hz at tricuspid vs pulmonary locations.

The left graph and right graph include the 0-100 Hz frequency range and address the tricuspid and pulmonary location for each of the 24 subjects. The subject number varies across the x-axis and the mean S1/S2 ratio varies across the y-axis. In this instance, as seen in the left graph of Figure 17, Subject 1 has a mean S1/S2 ratio of 1.0568 at the tricuspid sensor and a mean S1/S2 ratio of 0.806 at the pulmonary sensor. This is a difference of 0.2508, as seen in the right graph for Subject 1. In this PCG full range, 20/24 subjects have a greater tricuspid mean S1/S2 ratio than pulmonary mean S1/S2 ratio.

Additionally, the t-test returned a p-value of 5.22E-05 for the mean S1/S2 difference between the tricuspid and pulmonary location. This is significant, where $p \leq 0.05$. This is

expected because these locations are relatively spatially far apart. It may be interpreted that their difference in ratios is due to their locational difference rather than due to chance alone.

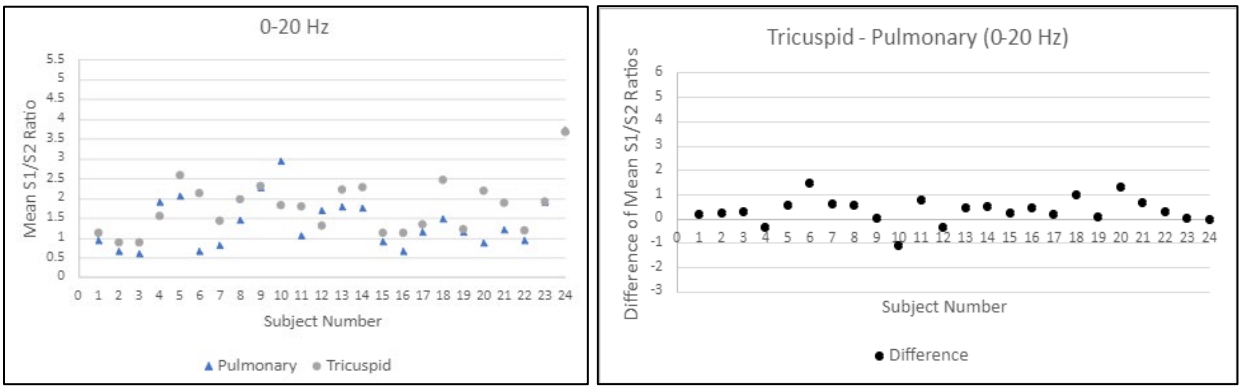

Figure 18: Mean S1/S2 ratio (left) and difference of mean S1/S2 ratio (right) in 0-20 Hz at tricuspid vs pulmonary locations.

In the PCG subaudible range, 19/24 subjects have a greater tricuspid mean S1/S2 ratio than pulmonary mean S1/S2 ratio. The p-value is significant at 0.009.

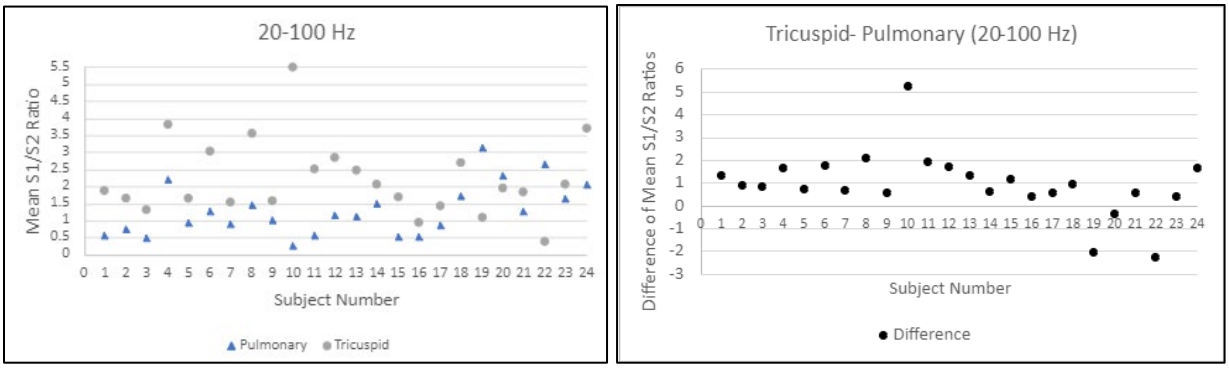

Figure 19: Mean S1/S2 ratio (left) and difference of mean S1/S2 ratio (right) in 20-100 Hz at tricuspid vs pulmonary locations.

In the PCG audible range, 21/24 subjects have a greater tricuspid mean S1/S2 ratio than pulmonary mean S1/S2 ratio. The p-value is significant at 0.004.

Because S1 is believed to be generated at inferior locations and S2 at superior locations of the heart [12], it expected that the S1/S2 ratio would be greater at inferior locations. In Figure 19,

21 of the 24 subjects have a difference of mean S1/S2 ratio > 0 between the tricuspid and pulmonary location. Of note, there are three subjects (19, 20, and 22) that did not follow the trend described. This is surprising, considering this trend is taken to be commonplace and expected. Several data points (BMI and self-reported cardiac health) were taken into consideration as possible explanations to explain why these subjects' results differed from the others.

Subject 19 is a female, with a BMI of 23.6 which is classified as "normal weight." She did not report a history of cardiac conditions. Subject 20 is a male, with a BMI of 19.8 which is classified as "normal weight." He did not report a history of cardiac conditions. Subject 22 is a female, with a BMI of 30.4, which is classified as "obese." This excess weight may contribute to increased chest surface tissue that would inhibit the ability of the sensors in some capacity. Regarding cardiac conditions, the subject did not provide information on a personal or family history of cardiac issues. This is because the information was deemed optional on the form the participants filled out. It is possible that this subject had a cardiac condition which contributed to not following the trend. However, this is merely speculation, and it is difficult to point to explanations for all three of these subjects' differences.

Nonetheless, Figure 19 still indicates that the inferior location generally had a greater mean S1/S2 ratio, which is expected. Therefore, this accomplishes the first goal outlined in Section 3.1, which is to "confirm spatial distribution results of the measured audible heart sounds (as measured by S1/S2 ratio with PCG sensors) and compare these results with the literature." This provides confidence in the study methods and sensors.

4.1.2 PCG - Aortic vs Pulmonary for All three Frequency Ranges

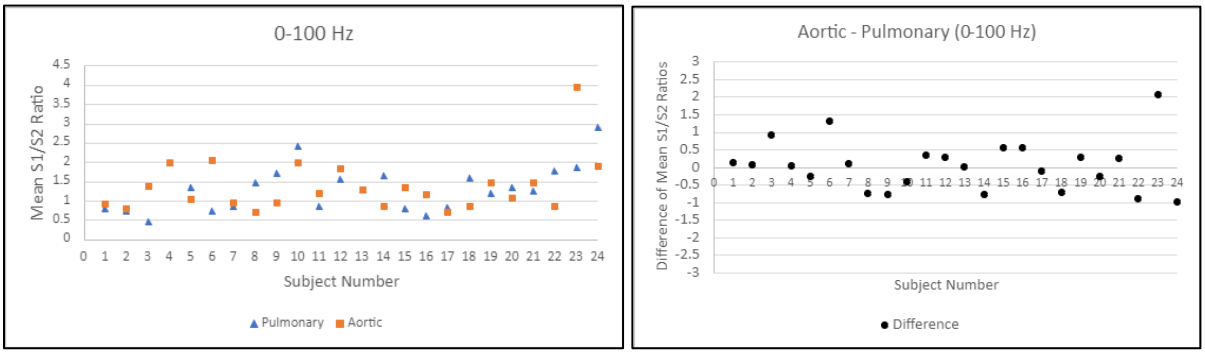

Figure 20: Mean S1/S2 ratio (left) and difference of mean S1/S2 ratio (right) in 0-100 Hz at aortic vs pulmonary locations.

In the PCG full range, 13/24 subjects have a greater aortic mean S1/S2 ratio than pulmonary mean S1/S2 ratio. The p-value is not significant at 0.842.

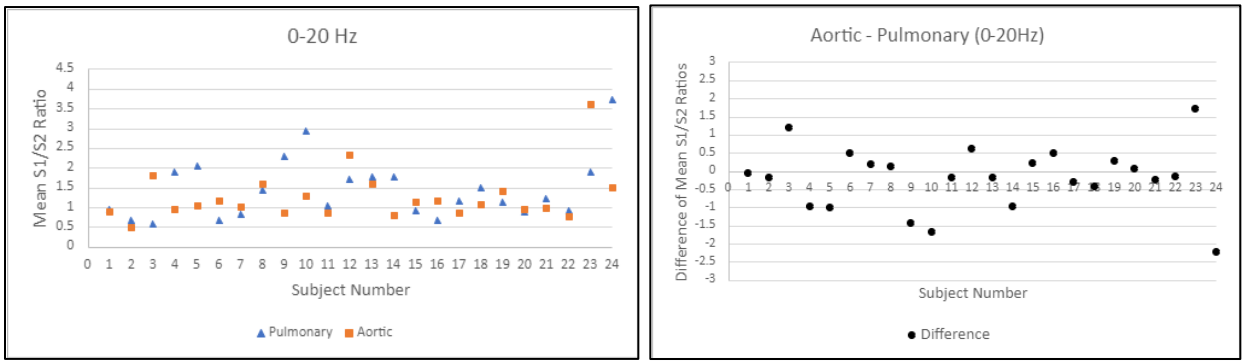

Figure 21: Mean S1/S2 ratio (left) and difference of mean S1/S2 ratio (right) in 0-20 Hz at aortic vs pulmonary locations.

In the PCG subaudible range, 10/24 subjects have a greater aortic mean S1/S2 ratio than pulmonary mean S1/S2 ratio. The p-value is not significant at 0.292.

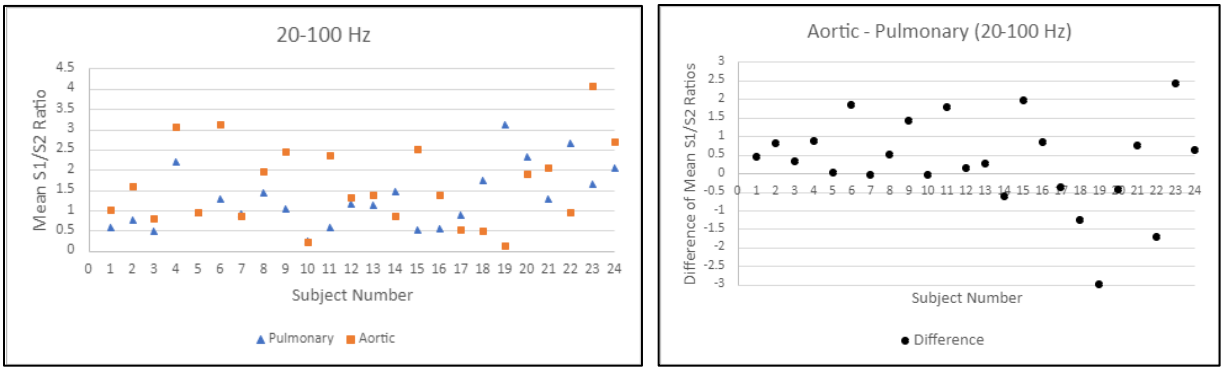

Figure 22: Mean S1/S2 ratio (left) and difference of mean S1/S2 ratio (right) in 20-100 Hz at aortic vs pulmonary locations.

In the PCG audible range, 16/24 subjects have a greater aortic mean S1/S2 ratio than pulmonary mean S1/S2 ratio. The p-value is not significant at 0.218.

4.1.3 PCG - Tricuspid vs Aortic for All Three Frequency Ranges

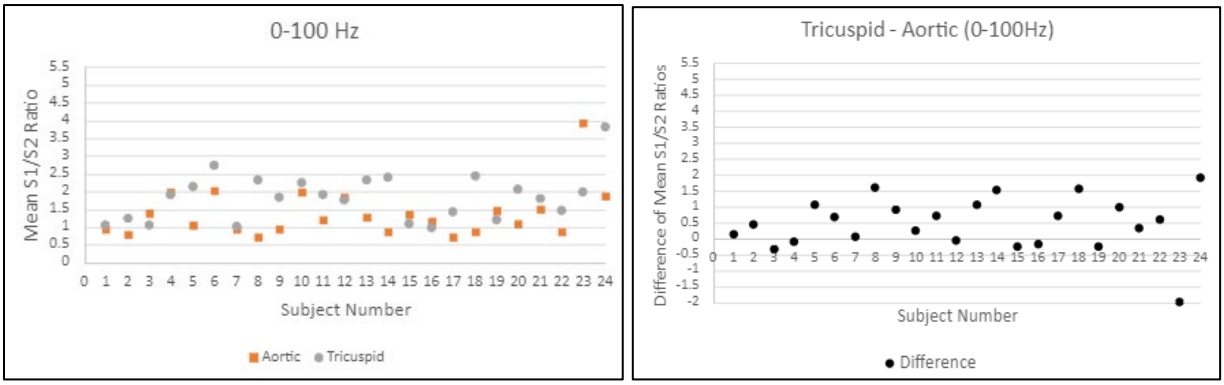

Figure 23: Mean S1/S2 ratio (left) and difference of mean S1/S2 ratio (right) in 0-100 Hz at tricuspid vs aortic locations.

In the PCG full range, 17/24 subjects have a greater tricuspid mean S1/S2 ratio than aortic mean S1/S2 ratio. The p-value is significant at 0.011.

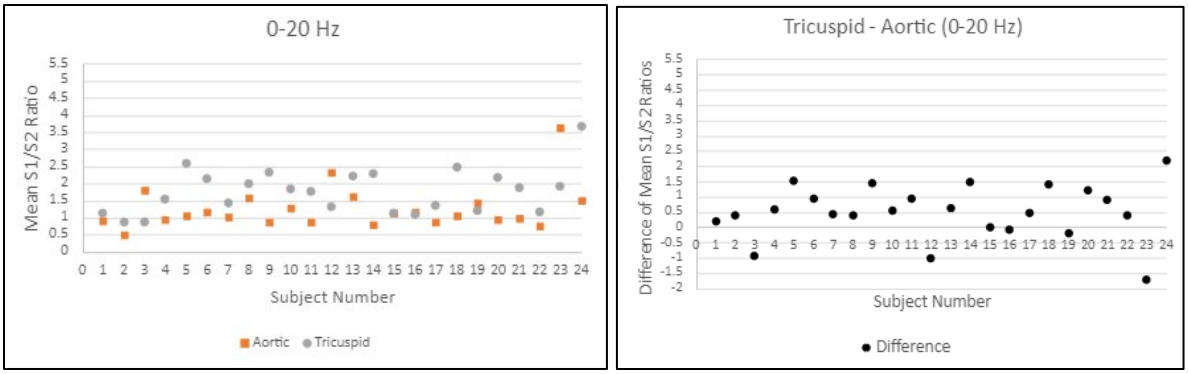

Figure 24: Mean S1/S2 ratio (left) and difference of mean S1/S2 ratio (right) in 0-20 Hz at tricuspid vs aortic locations.

In the PCG subaudible range, 18/24 subjects have a greater tricuspid mean S1/S2 ratio than aortic mean S1/S2 ratio. The p-value is significant at 0.010.

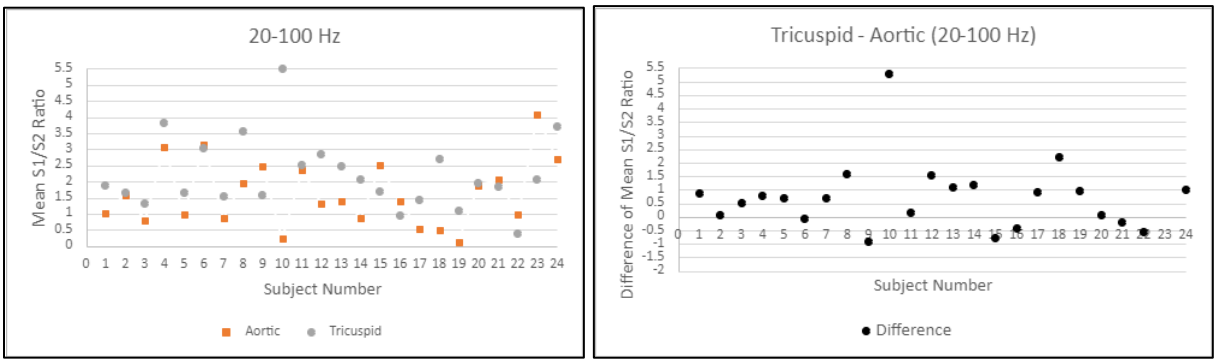

Figure 25: Mean S1/S2 ratio (left) and difference of mean S1/S2 ratio (right) in 20-100 Hz at tricuspid vs aortic locations.

In the PCG audible range, 17/24 subjects have a greater tricuspid mean S1/S2 ratio than aortic mean S1/S2 ratio. The p-value is significant at 0.041.

Below are three tables that provide a summary of the key data points from sections 4.1.1, 4.1.2, and 4.1.3.

Table 2: Summary of PCG data for tricuspid vs pulmonary locations

Frequency Range	Number of subjects (of 24 total) with a "difference of mean S1/S2 ratio" > 0	P-value	Significant?
0-100 Hz	20	5.22E-0	Yes
0-20 Hz	19	0.009	Yes
20-100 Hz	21	0. 0040	Yes

Table 3: Summary of PCG data for aortic vs pulmonary locations

Frequency Range	Number of subjects (of 24 total) with a "difference of mean S1/S2 ratio" > 0	P-value	Significant?
0-100 Hz	13	0.842	No
0-20 Hz	10	0.292	No
20-100 Hz	16	0.218	No

Table 4: Summary of PCG data for tricuspid vs aortic locations

Frequency Range	Number of subjects (of 24 total) with a "difference of mean S1/S2 ratio" > 0	P-value	Significant?
0-100 Hz	17	0.011	Yes
0-20 Hz	18	0.010	Yes
20-100 Hz	17	0.041	Yes

4.2 Seismocardiography Data

Three sensor locations were studied for this seismocardiography-only section: pulmonary, tricuspid, and "LCE." While LCE, or "laterally contiguous to Erb's point" is not a traditional auscultation location, it was used in this study because of its proximity to other

sensors and is placed just lateral to Erb's point, which is at the LCE. It was given this abbreviation to be descriptive because no formal name is given to it in the literature. The plots on the left side of the page indicate the mean S1/S2 ratio for two locations, for each subject. The plots on the right side of the page are based on the plots on the left. The right-sided plots indicate the *difference* in mean S1/S2 ratio of two locations for each subject.

Additionally, to account for three different frequency ranges of interest (see Table 1), a total of six plots were generated for each two locations compared against each other. T-tests were applied to determine p-value, which indicates the significance in the difference of mean SCG1/SCG2 ratio between locations. The number of subjects (out of the 24 total) that had a "difference of mean SCG1/SCG2 ratio" > 0 was also included for analysis as another quantitative measurement.

4.2.1 SCG –Tricuspid vs Pulmonary for All Three Frequency Ranges

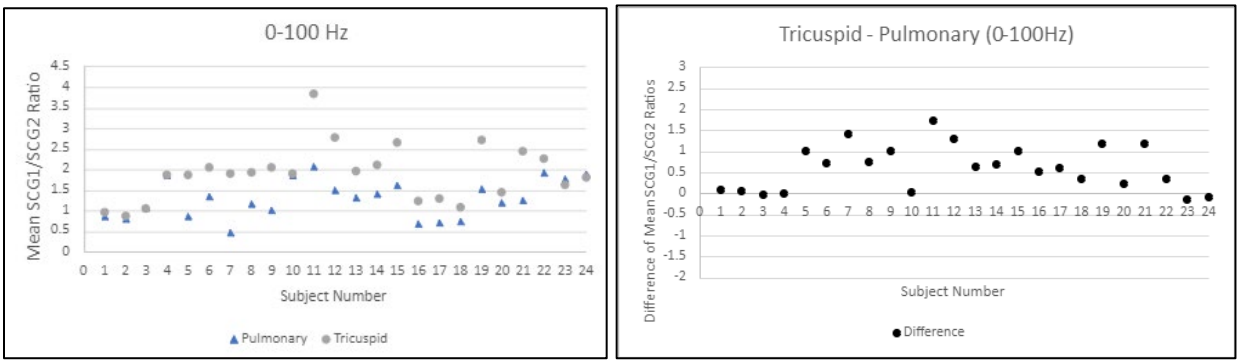

Figure 26: Mean SCG1/SCG2 ratio (left) and difference of mean SCG1/SCG2 ratio (right) in 0-100 Hz at pulmonary vs tricuspid locations.

In the SCG full range, 21/24 subjects have a greater tricuspid mean SCG1/SCG2 ratio than pulmonic mean SCG1/SCG2 ratio. The p-value is significant at 1.22E-05.

In this full range instance, the SCG Mean S1/S2 Ratio is generally positive (in 21/24 subjects), which is similar to the PCG's full range comparison of Tricuspid vs Pulmonary with 20/24 ratios being positive. This suggests that PCG and SCG behave similarly in the audible range. PCG and SCG will be further compared in section 4.3.

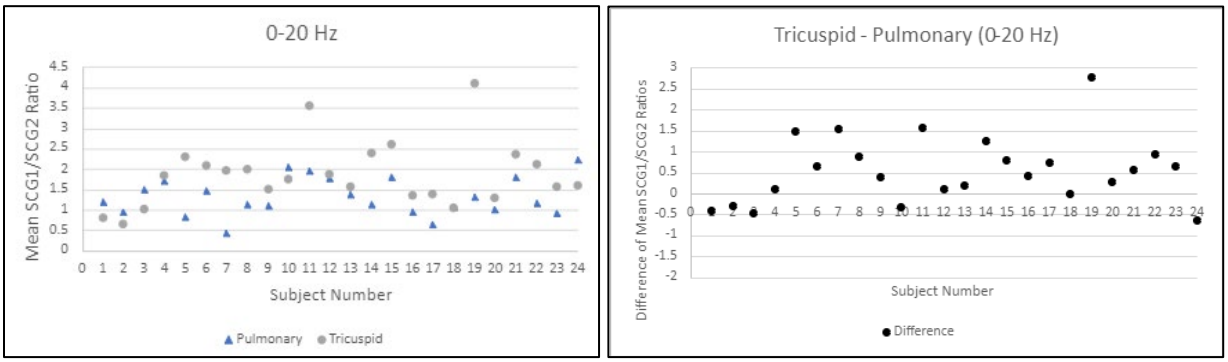

Figure 27: Mean SCG1/SCG2 ratio (left) and difference of mean SCG1/SCG2 ratio (right) in 0-20 Hz at tricuspid vs pulmonary locations.

In the SCG subaudible range, 18/24 subjects have a greater tricuspid mean SCG1/SCG2 ratio than pulmonic mean SCG1/SCG2 ratio. The p-value is significant at 0.0006.

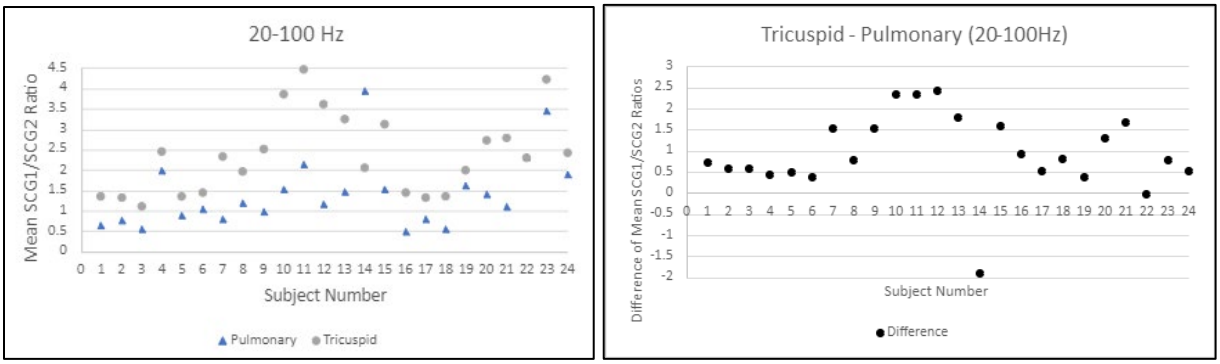

Figure 28: Mean SCG1/SCG2 ratio (left) and difference of mean SCG1/SCG2 ratio (right) in 20-100 Hz at tricuspid vs pulmonary locations.

In the SCG audible range, 22/24 subjects have a greater tricuspid mean SCG1/SCG2 ratio than pulmonic mean SCG1/SCG2 ratio. The p-value is significant at 5.32E-05.

4.2.2 SCG – LCE vs Pulmonary for All Three Frequency Ranges

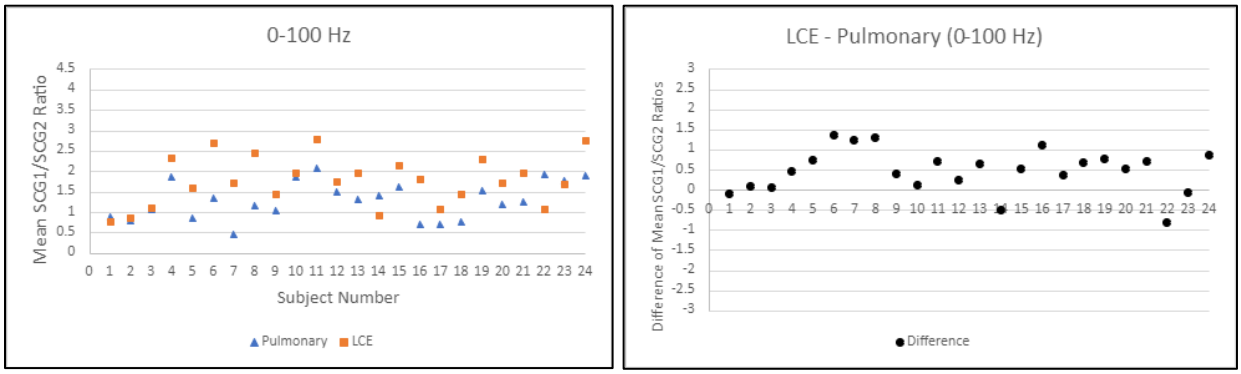

Figure 29: Mean SCG1/SCG2 ratio (left) and difference of mean SCG1/SCG2 ratio (right) in 0-100 Hz at LCE vs pulmonary locations.

In the SCG full range, 20/24 subjects have a greater LCE mean SCG1/SCG2 ratio than pulmonic mean SCG1/SCG2 ratio. The p-value is significant at 0.0003.

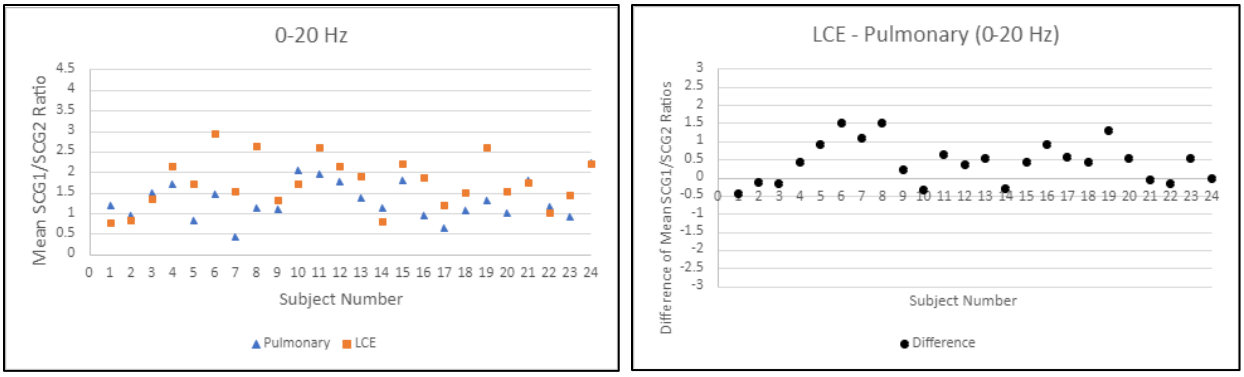

Figure 30: Mean SCG1/SCG2 ratio (left) and difference of mean SCG1/SCG2 ratio (right) in 0-20 Hz at LCE vs pulmonary locations.

In the SCG subaudible range, 16/24 subjects have a greater LCE mean SCG1/SCG2 ratio than pulmonic mean SCG1/SCG2 ratio. The p-value is significant at 0.001.

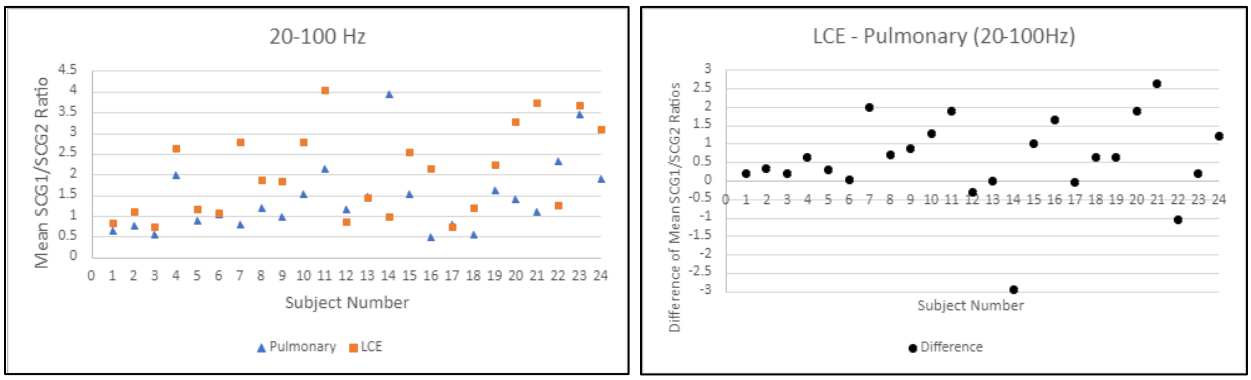

Figure 31: *Mean SCG1/SCG2 ratio (left) and difference of mean SCG1/SCG2 ratio (right) in 20-100 Hz at LCE vs pulmonary locations.*

In the SCG audible range, 19/24 subjects have a greater LCE mean SCG1/SCG2 ratio than pulmonic mean SCG1/SCG2 ratio. The p-value is significant at 0.022.

4.2.3 SCG - Tricuspid vs LCE for All Three Frequency Ranges

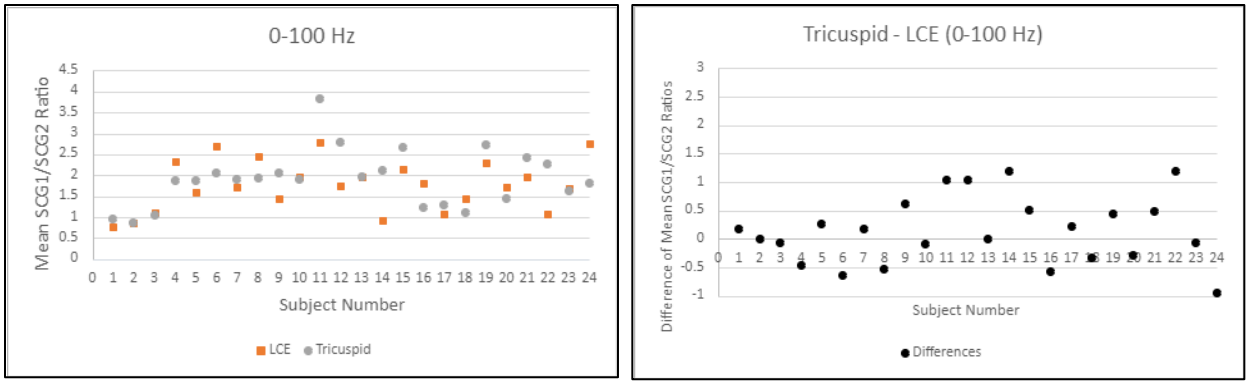

Figure 32: *Mean SCG1/SCG2 ratio (left) and difference of mean SCG1/SCG2 ratio (right) in 0-100 Hz at LCE vs tricuspid locations.*

In the SCG full range, 13/24 subjects have a greater tricuspid mean SCG1/SCG2 ratio than LCE mean SCG1/SCG2 ratio. The p-value is insignificant at 0.269.

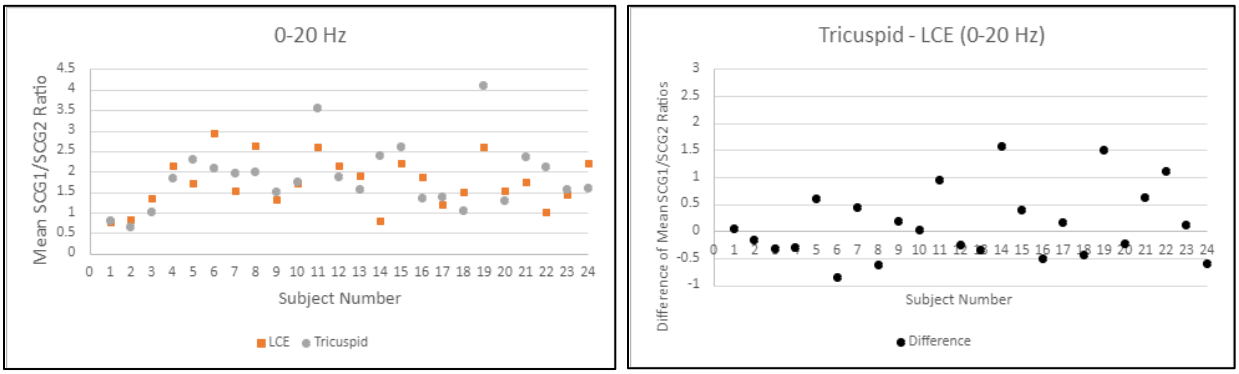

Figure 33: Mean SCG1/SCG2 ratio (left) and difference of mean SCG1/SCG2 ratio (right) in 0-20 Hz at LCE vs tricuspid locations.

In the SCG subaudible range, 13/24 subjects have a greater tricuspid mean SCG1/SCG2 ratio than LCE mean SCG1/SCG2 ratio. The p-value is insignificant at 0.365.

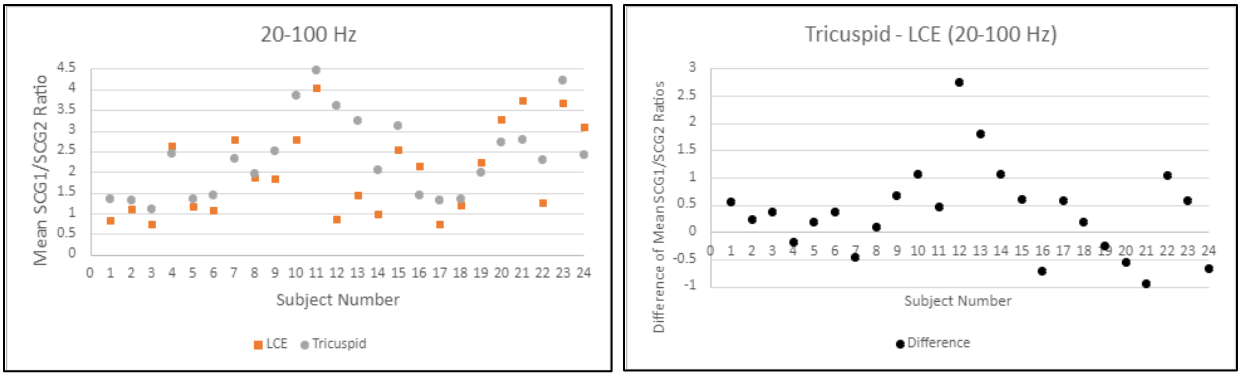

Figure 34: Mean SCG1/SCG2 ratio (left) and difference of mean SCG1/SCG2 ratio (right) in 20-100 Hz at LCE vs tricuspid locations.

In the SCG audible range, 17/24 subjects have a greater tricuspid mean SCG1/SCG2 ratio than LCE mean SCG1/SCG2 ratio. The p-value is significant at 0.044.

Below are three tables that provide a summary of the key data points from sections 4.2.1, 4.2.2, and 4.2.3.

Table 5: Summary of SCG data for tricuspid vs pulmonary locations

Frequency Range	Number of subjects (of 24 total) with a "difference of mean S1/S2 ratio" > 0	P-value	Significant?
0-100 Hz	21	1.22E-05	Yes
0-20 Hz	18	0.0006	Yes
20-100 Hz	22	5.32E-05	Yes

Table 6: Summary of SCG data for LCE vs pulmonary locations

Frequency Range	Number of subjects (of 24 total) with a "difference of mean S1/S2 ratio" > 0	P-value	Significant?
0-100 Hz	20	0.0003	Yes

0-20 Hz	16	0.001	Yes
20-100 Hz	19	0.022	Yes

Table 7: Summary of SCG data for tricuspid vs LCE locations

Frequency Range	Number of subjects (of 24 total) with a "difference of mean S1/S2 ratio" > 0	P-value	Significant?
0-100 Hz	13	0.269	No
0-20 Hz	13	0.365	No
20-100 Hz	17	0.044	Yes

4.3 Comparison of Phonocardiography and Seismocardiography Data

This section compares PCG sensor signals (mean S1/S2 ratio) and SCG sensor signals (mean SCG1/SCG2 ratio) at the same location, repeated for three locations. The data was not recorded at the same time but rather in back-to-back recording sessions. All three frequency ranges are utilized again.

4.3.1 Comparison of PCG vs SCG at Pulmonary Location for All Three Frequency Ranges

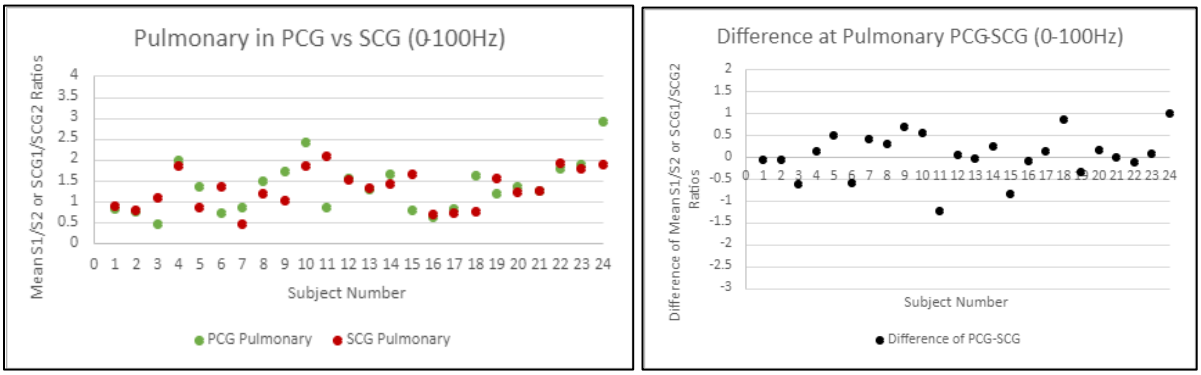

Figure 35: Mean S1/S2 or SCG1/SCG2 ratio (left) and difference of mean S1/S2 or SCG1/SCG2 ratio (right) in 0-100 Hz at the pulmonary location.

In the full range, 13/24 subjects have a greater mean SCG1/SCG2 ratio than mean S1/S2 ratio at the pulmonary location. The p-value is insignificant at 0.696.

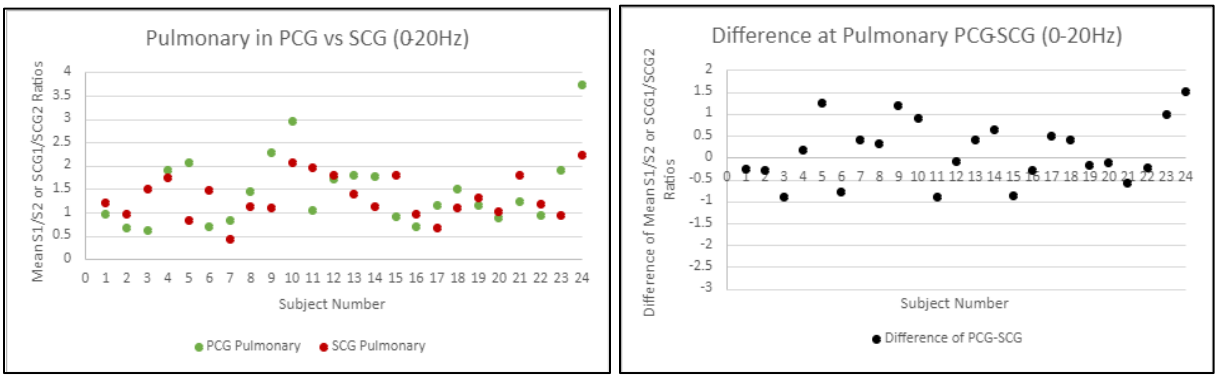

Figure 36: Mean S1/S2 or SCG1/SCG2 ratio (left) and difference of mean S1/S2 or SCG1/SCG2 ratio (right) in 0-20 Hz at the pulmonary location.

In the subaudible range, 11/24 subjects have a greater mean SCG1/SCG2 ratio than mean S1/S2 ratio at the pulmonary location. The p-value is insignificant at 0.376.

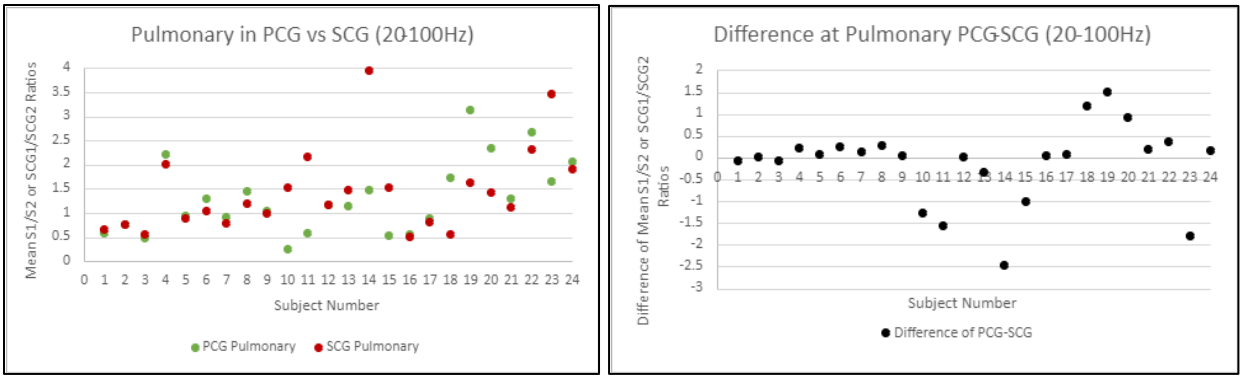

Figure 37: Mean S1/S2 or SCG1/SCG2 ratio (left) and difference of mean S1/S2 or SCG1/SCG2 ratio (right) in 20-100 Hz at the pulmonary location.

In the audible range, 14/24 subjects have a greater mean SCG1/SCG2 ratio than mean S1/S2 ratio at the pulmonary location. The p-value is insignificant at 0.474.

4.3.2 Comparison of PCG vs SCG at Erb's Point for All Three Frequency Ranges

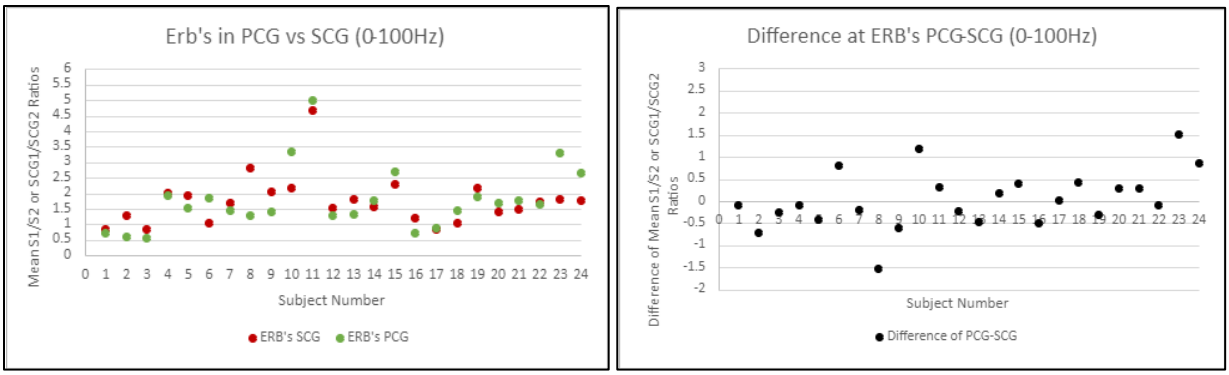

Figure 38: Mean S1/S2 or SCG1/SCG2 ratio (left) and difference of mean S1/S2 or SCG1/SCG2 ratio (right) in 0-100 Hz at Erb's point.

In the full range, 11/24 subjects have a greater mean SCG1/SCG2 ratio than mean S1/S2 ratio at the Erb's location. The p-value is insignificant at 0.837.

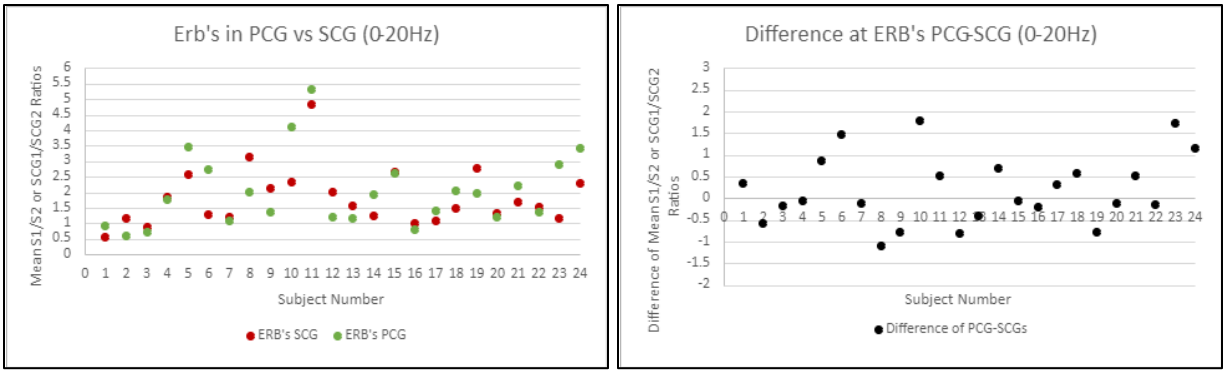

Figure 39: Mean S1/S2 or SCG1/SCG2 ratio (left) and difference of mean S1/S2 or SCG1/SCG2 ratio (right) in 0-20 Hz at Erb's point.

In the subaudible range, 11/24 subjects have a greater mean SCG1/SCG2 ratio than mean S1/S2 ratio at the Erb's location. The p-value is insignificant at 0.256.

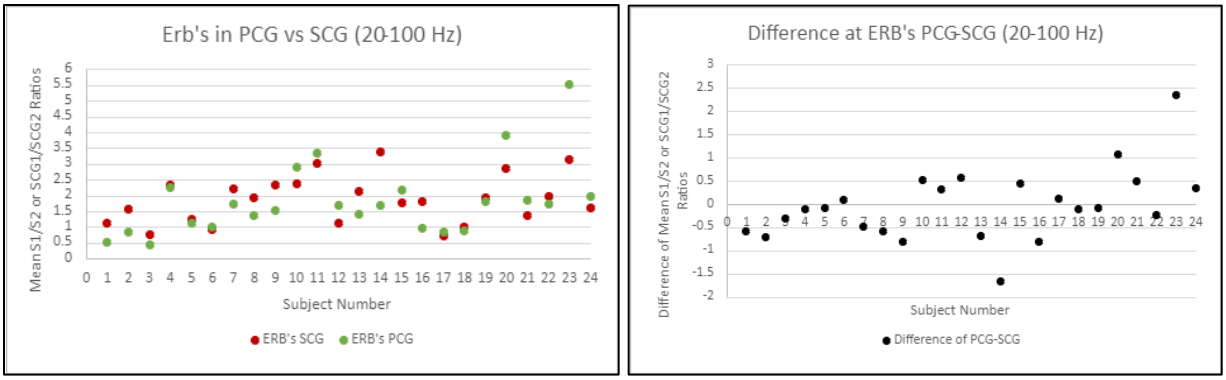

Figure 40: Mean S1/S2 or SCG1/SCG2 ratio (left) and difference of mean S1/S2 or SCG1/SCG2 ratio (right) in 20-100 Hz at Erb's point.

In the audible range, 10/24 subjects have a greater mean SCG1/SCG2 ratio than mean S1/S2 ratio at the Erb's location. The p-value is insignificant at 0.783.

4.3.3 Comparison of PCG vs SCG at Tricuspid Location for All Three Frequency Ranges

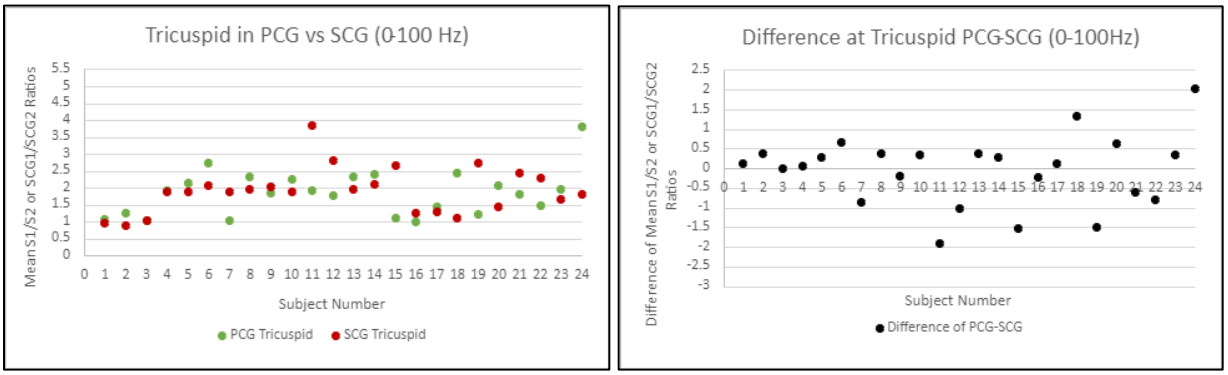

Figure 41: Mean S1/S2 or SCG1/SCG2 ratio (left) and difference of mean S1/S2 or SCG1/SCG2 ratio (right) in 0-100 Hz at the tricuspid location.

In the full range, 13/24 subjects have a greater mean SCG1/SCG2 ratio than mean S1/S2 ratio at the tricuspid location. The p-value is insignificant at 0.742.

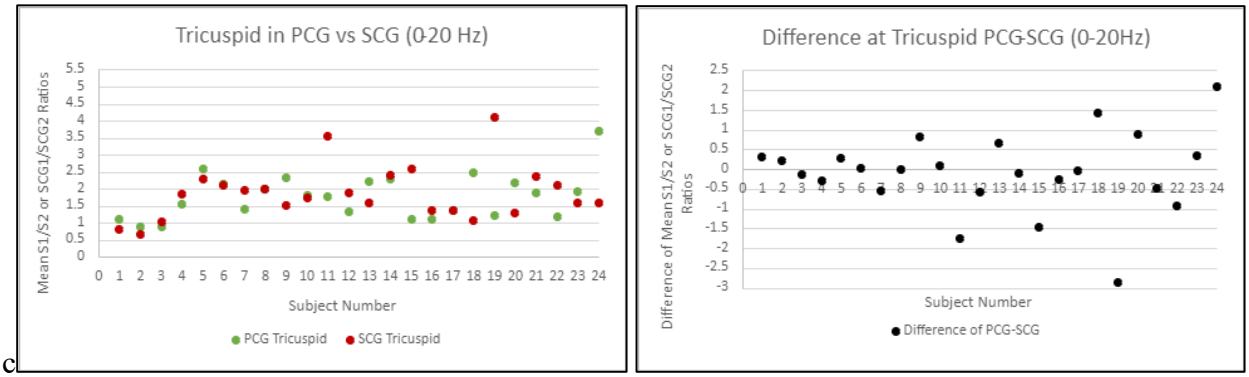

c

Figure 42: Mean S1/S2 or SCG1/SCG2 ratio (left) and difference of mean S1/S2 or SCG1/SCG2 ratio (right) in 0-20 Hz at the tricuspid location.

In the subaudible range, 14/24 subjects have a greater mean SCG1/SCG2 ratio than mean S1/S2 ratio at the tricuspid location. The p-value is insignificant at 0.636.

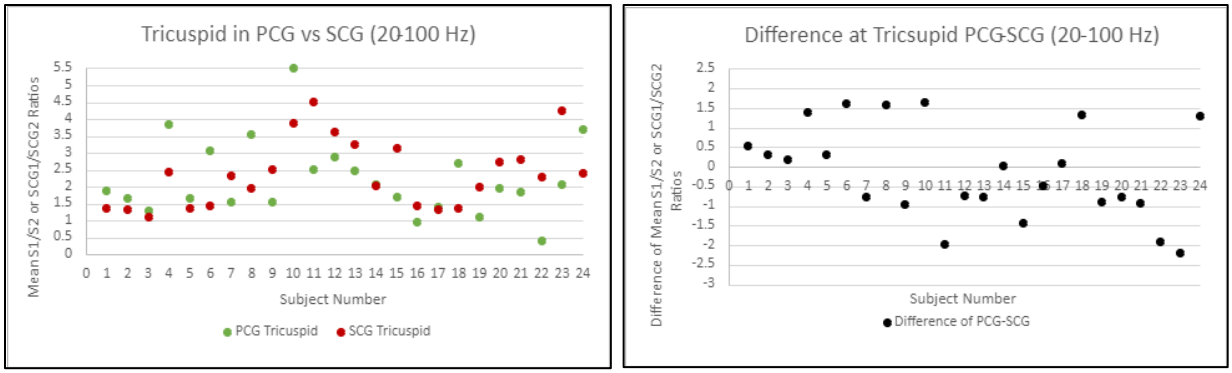

Figure 43: Mean S1/S2 or SCG1/SCG2 ratio (left) and difference of mean S1/S2 or SCG1/SCG2 ratio (right) in 20-100 Hz at the tricuspid location.

In the audible range, 11/24 subjects have a greater mean SCG1/SCG2 ratio than mean S1/S2 ratio at the tricuspid location. The p-value is insignificant at 0.550.

From a visual perspective alone, the audible cases do not seem to show a discernable trend between PCG sensor and SCG sensor points. This is similarly the case for subaudible cases. Rather, neither the PCG sensor results nor SCG have a consistently higher S1/S2 ratio in either frequency range. The tables below provide quantifiable data to support what is visualized in the plots.

Table 8: Number of subjects (of 24 total) with a "difference of mean S1/S2 ratio" > 0

	0-100 Hz	0-20 Hz	20-100 Hz
Pulmonary	13	11	14
Erb's Point	11	11	10
Tricuspid	13	14	11

Table 9: P-values for PCG vs SCG for three frequency ranges at three locations

	0-100 Hz	0-20 Hz	20-100 Hz
Pulmonary	0.696	0.376	0.474
Erb's Point	0.837	0.256	0.783
Tricuspid	0.742	0.636	0.550

Table 10: Standard Deviations for Difference Between PCG and SCG in three frequency ranges and three locations

	0-100 Hz	0-20 Hz	20-100 Hz
Pulmonary	0.519	0.706	0.908
Erb's Point	0.652	0.800	0.783
Tricuspid	0.900	1.02	1.19

Firstly, the focus will be on interpreting the p-value within a single cell, such as the cell at the intersection of pulmonary row and 20-100 Hz column. The insignificance of this p-value is reassuring because it is expected. It signifies that the PCG sensor and SCG sensor at the same location did not detect differences in S1/S2 in any discernable trend or pattern, but rather randomly. This suggests that the PCG sensor and SCG sensors are detecting similar data when at the same location.

Secondly, the p-values will be compared at different frequency ranges yet within the same location. When subaudible and audible cases are compared, the p-values (p) are insignificant across all locations (Table 9). Although the degree to how "insignificant" they are

in terms of p-value varies, they are all reasonably insignificant when considering $p \leq 0.05$ to be significant. The closest to significant would be the subaudible range of Erb's point at 0.256.

Thirdly, the STD values between frequency ranges at the same location will be considered. When looking across a row for a particular location, it can be seen that the subaudible and audible ranges are similar in terms of STD (Table 10). The standard deviation differences between subaudible and audible of Erb's point, for instance, is only approximately 0.016. This indicates that there is a similar distribution of differences between PCG mean S1/S2 ratio and SCG mean SCG1/SCG2 ratio for one location.

These second and third topics of discussion underscore interesting results. Initially, it was expected that SCG sensor and PCG sensor may disagree in the subaudible range because SCG is known to be capable of detecting subaudible frequencies better than a PCG sensor. However, it seems that the agreement between PCG sensor and SCG sensor in both subaudible and audible bands is comparable when S1/S2 ratio is used as the metric. This is likely because the carefully selected, high-quality PCG sensor used in this study was able to detect some subaudible frequencies. This results in both sensors detecting similar data although that was not the original intent of the PCG sensor. This is further explored in Section 4.3.4.

An initial, plausible prediction was that the full range would appear to be a "middle-ground," or combination, between the subaudible and audible ranges. When considering STD, none of the three locations had a full range with a STD value between the subaudible and audible values. When comparing through the lens of p-value, the only case in which the full range p-value was in between the subaudible and audible was at the Tricuspid location.

4.3.4 Comparison of PCG Sensor vs SCG Sensor Regarding Waveforms and Frequency Content

Given the initial similarity between S1/S2 ratio results of the PCG sensor with the SCG1/SCG2 ratio results from the SCG sensor, another method was utilized to provide more information. Specifically, the waveform and frequency spectrum of a medoid beat were generated in MATLAB. The data was based on the two-minute normal breathing segment for both PCG and SCG sensor signals at the tricuspid location for Subject 1. The medoid is a representation of the "average" beat among all the beats in the data set. Figure 44 demonstrates the waveform (top plot) for a PCG sensor (a) and SCG sensor (b). The frequency spectrum is seen on the bottom plots of Figure 44. It is evident that the SCG signal carries a relatively greater amount of low-frequency signal, specifically in the 5-15 Hz range. However, the PCG sensor does detect frequencies below 20 Hz as seen in the spectrum plot, which may contribute to why the S1/S2 ratios between PCG and SCG sensors appeared to be similar in the subaudible range. Readers and researchers should be aware of this when consider explanations for the results.

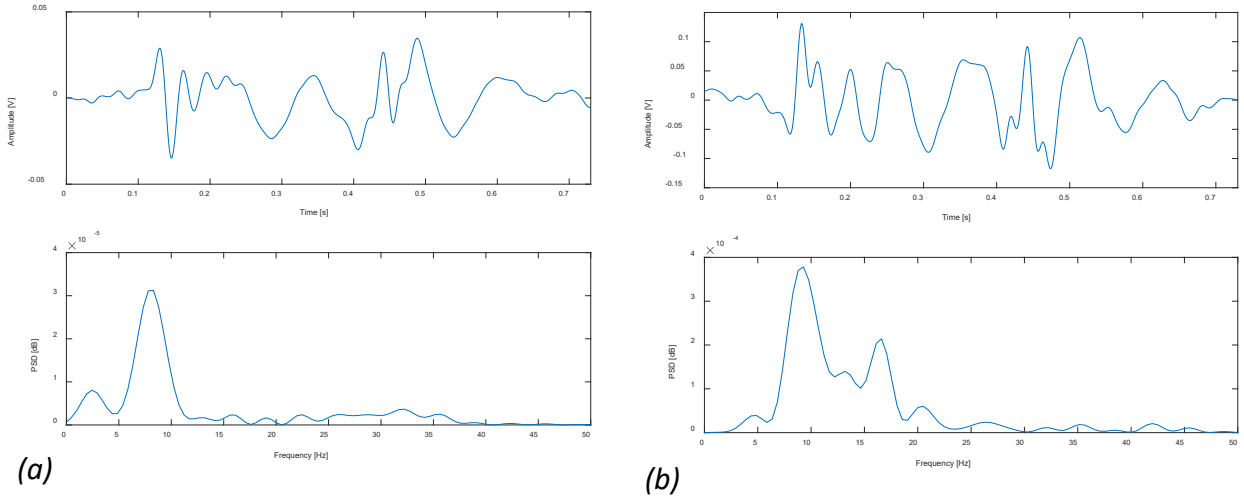

Figure 44: The waveform (top) and spectrum (bottom) from a PCG sensor (a) and SCG sensor (b) of a typical heartbeat at the tricuspid location. SCG appears to have relatively greater amount of low frequency content although low frequency content was detected by the PCG sensor.

Additionally, the the PCG sensor data was filtered to exclude frequencies below 20 Hz as seen in Figure 45. This is the visual representation of what clinicans may hear when listening to the audible heart sounds. It is evident that the waveforms of the two signals are significantly different, which suggests that there is information not detected when clinicans listen to audible heart sounds alone.

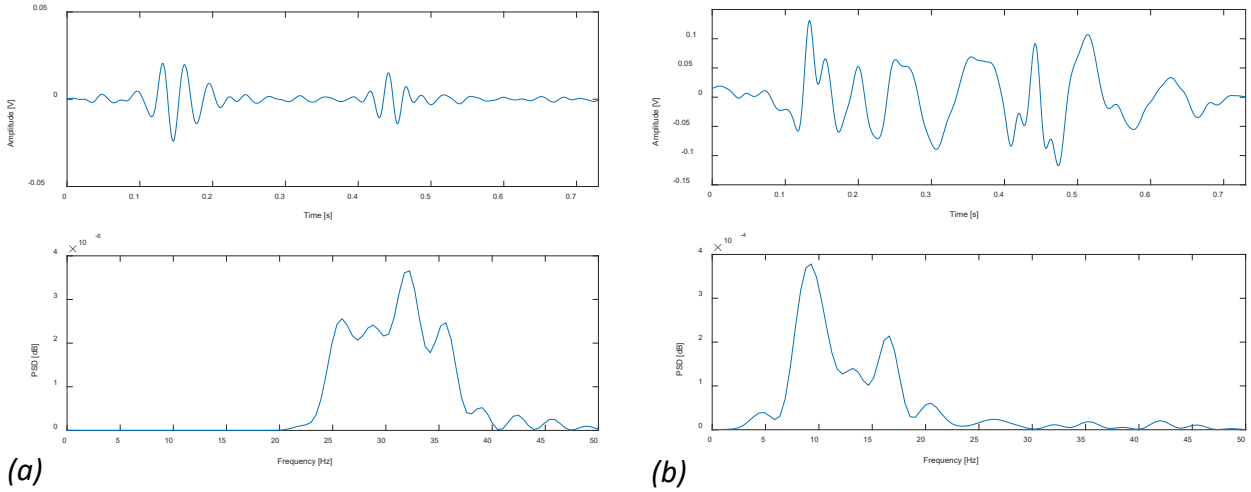

Figure 45: The waveform (top) and spectrum (bottom) from a PCG sensor (a) and SCG sensor (b) of a typical heartbeat at the tricuspid location. The PCG data was filtered to remove <20 Hz, which highlights the difference between audible HS and SCG.

A figure similar to Figure 45 was generated (Figure 46) but rather than the freequency spectrum on the bottom, a time frequency domain can be found. Once again, the subaudible components of the PCG sensor signal have been filtered out. The PCG sensor time frequency domain plot on the bottom illustrates relatively clear S1 and S2 events, near 0.15 and 0.45 seconds. It deserves clarifcation that although some frequency content appears to be less than 20 Hz in the PCG figure, it is due to leakage when filtering. This is in comparison to what the SCG sensor detects, on the right. Again, it is evident from from visual inspection that the SCG sensor offers far more data beyond what can be heard, including in between S1 and S2 as well as

subaudibly. This finding warrants further investigation, possibly using additional metrics to better understand the nuances in their distinction and the clinical interperation.

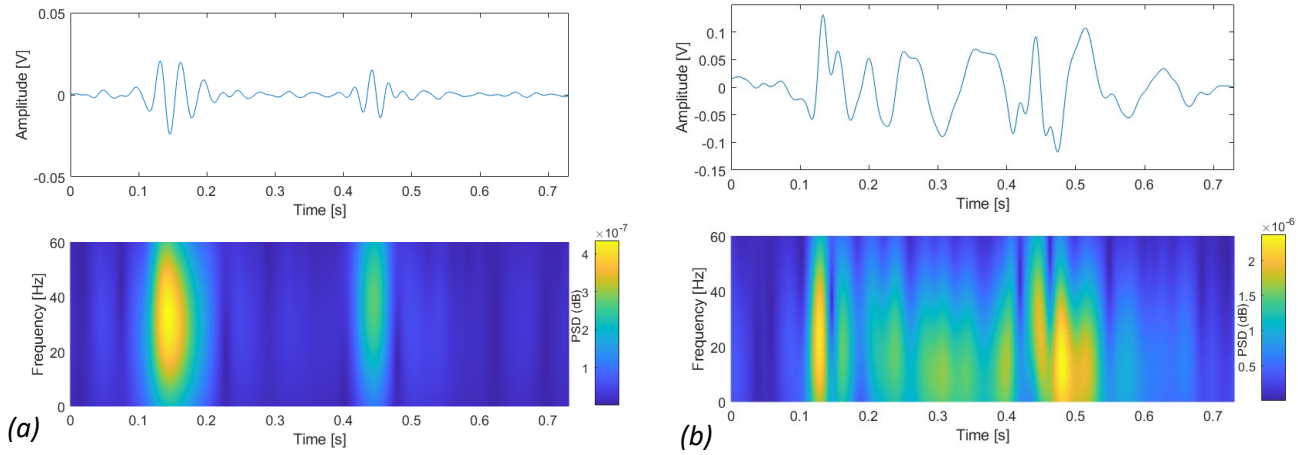

Figure 46: The waveform (top) and time frequency domain (bottom) from a PCG sensor (a) and SCG sensor (b) of a typical heartbeat at the tricuspid location. The PCG sensor signal included filtering out frequencies below 20 Hz. Low frequency content is found more plentifully in the SCG sensor and would not be only listening to heart sounds (left).

Figure 47 is provided as a comparison to Figure 46 (a) because it provided the non-filtered PCG sensor results. It is evident that low-frequency components contribute to the waveform detected by the PCG sensor.

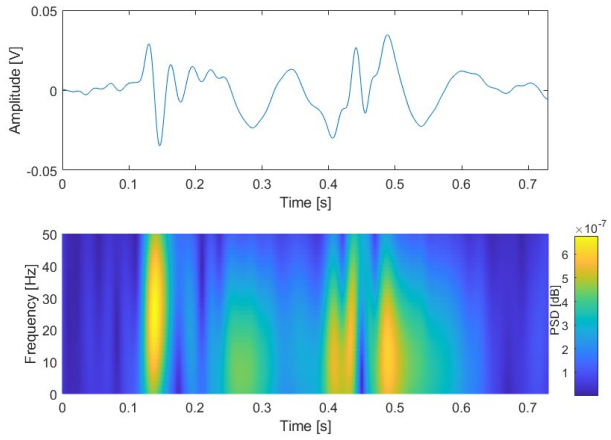

Figure 47: The waveform (top) and time frequency domain (bottom) from a PCG sensor of a typical heartbeat at the tricuspid location. The PCG sensor signal is not filtered.

Lastly, Figure 48 was generated to determine the frequency response of the PCG and SCG sensors. White noise (with frequency content ranging from 0-100 Hz) was generated from MATLAB and sent to a phantom surface, where the stethoscope and accelerometer were placed next to each other and their responses were collected. Although this figure is normalized, it is evident that in low frequencies, such as below 30 Hz, the response of the stethoscope and the accelerometer are remarkably similar. This was not initially expected but is likely because of the high-quality stethoscope sensor that was detected. While the original goal was to detect audible frequencies only, the stethoscope was able to detect subaudible frequencies quite well. However, when approaching relatively higher frequencies, such as 80 Hz, the stethoscope is more sensitive. This is expected, as stethoscopes are known to operate more sensitively in that range when compared to accelerometers. This figure may be the explanation regarding why the subaudible comparisons between PCG and SCG sensors yielded similar results.

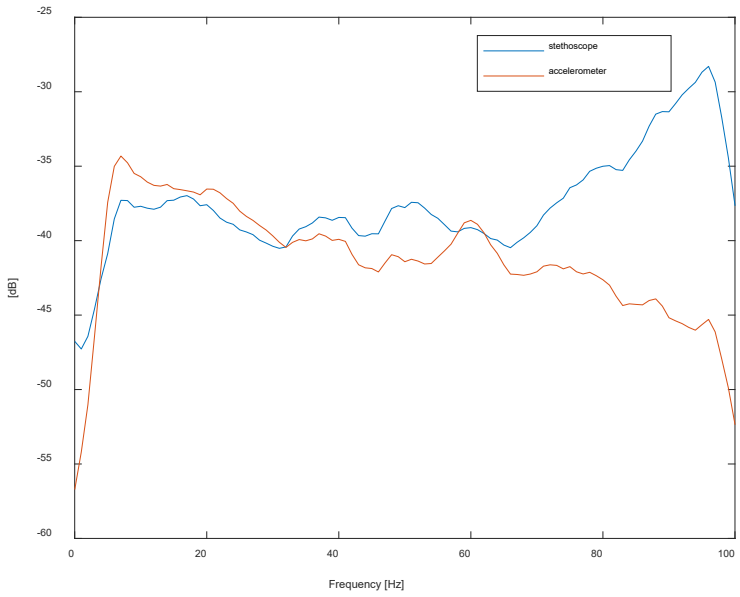

Figure 48: The normalized frequency response of the stethoscope (blue line) and the accelerometer (orange line) to the same output of white noise. The stethoscope detects low frequencies (<30 Hz) similarly to the accelerometer but deviates at higher frequencies (>80 Hz).

The non-normalized counterpart to Figure 48 was also generated and is seen as Figure 49.

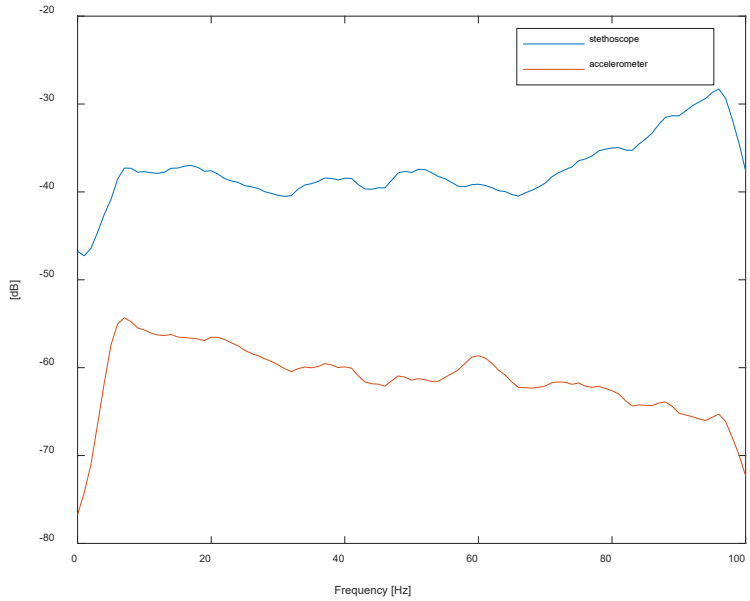

Figure 49: The non-normalized frequency response of the stethoscope (blue line) and the accelerometer (orange line) to the same output of white noise.

CHAPTER 5: CONCLUSIONS

This study examined the relationship between PCG and SCG mainly using the metric of the mean S1/S2 ratio and in different frequency bands. The results point to two overall conclusions:

1) The S1/S2 mean ratio and SCG1/SCG2 mean ratio is higher in inferior locations when compared to superior. This is seen in tricuspid vs pulmonary locations. This is expected and the PCG-sensor-specific aspect confirms current literature.
2) The second conclusion is about the relationship between PCG and SCG. The figures regarding S1/S2 ratio, standard deviation and p-value tables in Chapter 4 illustrate that the PCG sensor and SCG sensor are comparable, even in the subaudible range. This is likely because the PCG sensor also detects low-frequency content rather than the audible heart sounds alone. However, when PCG data is filtered to include audible heart sounds only, it reinforces the important distinction between SCG and what clinicians detect.

Additionally, the significance between comparisons provides another perspective and are listed together below for easy reference:

- PCG sensor only: See Table 11. In the graphs, “yes” corresponds to a p-value that is significant whereas “no” corresponds to a p-value that is not significant. All three frequencies bands of “Tricuspid vs Pulmonary” and “Tricuspid vs Aortic” were significant. All three frequencies bands of “Aortic vs Pulmonary” were not significant. This is likely because the aortic and pulmonary locations are in the same intercostal space and any differences in heart sounds are apparently not striking enough to be significantly detected by the PCG sensors,

Table 11: Binary Significance (based on p-values) of PCG Comparisons at Three Locations and Three Frequency Bands

	0-100 Hz	0-20 Hz	20-100 Hz
Tricuspid vs Pulmonary	Yes	Yes	Yes
Tricuspid vs Aortic	Yes	Yes	Yes
Aortic vs Pulmonary	No	No	No

- SCG only: See Table 12. All three frequencies bands of "Tricuspid vs Pulmonary" and "LCE vs pulmonary" were significant. 2/3 frequencies bands (full, subaudible) of "Tricuspid vs LCE" were not significant. Once again, it seems that the distance between sensors plays a role in significance and the tricuspid and LCE locations are likely not far enough for a significant difference to be detected in their heart sounds.

Table 12: Binary Significance (based on p-values) of SCG Comparisons at Three Locations and Three Frequency Bands

	0-100 Hz	0-20 Hz	20-100 Hz
Tricuspid vs Pulmonary	Yes	Yes	Yes
LCE vs Pulmonary	Yes	Yes	Yes
Tricuspid vs LCE	No	No	Yes

- PCG vs SCG: When the same location was compared between a PCG and SCG sensor, differences in S1/S2 were not significant for all frequency ranges of each location (Pulmonary, Erb's, Tricuspid). This is reassuring because it suggests that the PCG sensor and SCG sensor are detecting and reporting the same heart sounds.

Table 13: Binary Significance (based on p-values) of PCG vs SCG Comparisons at Three Locations and Three Frequency Bands

	0-100 Hz	0-20 Hz	20-100 Hz
Pulmonary	No	No	No
Erb's	No	No	No
Tricuspid	No	No	No

A plethora of data has been collected and may be looked at through different lenses. Nonetheless, this provides a solid foundation for which to continue the work, which is explored with several suggestions in section 5.2 “Future Work.”

5.1 Limitations

As with most studies, there are certainly limitations to be addressed. Namely, there were 24 subjects analyzed in this thesis. However, a larger sample size would be beneficial to confirm and provide more confidence in trends already seen or point to new conclusions.

There was also a narrow range of ages of the studied subjects, mainly between age 18 to 24. Additionally, the “healthy” status of the subjects was self-reported and not evaluated by a cardiologist on site to determine cardiac health. Additionally, factors such as amount and most recent caffeine intake, medication use, chest surface density, and sex may play a role in the results that has not yet been elucidated.

5.2 Future Work

There are a variety of ways in which the work may be continued, including using the data that has already been collected and analyzed with MATLAB.

However, another avenue may be to investigate criteria beyond the S1/S2 or SCG1/SCG2 ratio. One of these other criteria may include morphology of the PCG and SCG signals. This can be done by filtering the PCG signal to exclude <20 Hz and compare this to SCG signal. This would better provide information on what clinicians do not detect by listening to heart sounds alone.

Additionally, although specific methods to accomplish this are still being considered, a comparison between signals may be facilitated by listening to how the recordings sound. This can be done initially with auditory comparison of a .wav file by human listeners without filtering. If background noise is disruptive, it is suggested to consider filtering to remove the noise. The frequency range may need to be adjusted to 30 Hz and above for better hearing. Criteria will need to be determined for an evaluator, or listener, to be trained in. This may include how similar recordings sound, possibly by asking which is higher or lower pitch.

Further, only the normal breathing portion of the recordings were analyzed. It is suggested to investigate data that was recorded with other breath patterns, such as slow and deep breathing or breath hold. This may be done to understand how respiration affects the PCG and SCG relationship.

When this future work is implemented, other metrics may have differing conclusions and are encouraged to be pursued to better discern the relationship between PCG and SCG. This is still the beginning of an exciting concept that warrants further study to determine how SCG may be a valuable tool to observe the heart's condition.

CHAPTER 6: REFERENCES

1. Centers for Disease Control and Prevention. Heart Disease. https://www.cdc.gov/heartdisease/index.htm. Published September 1, 2022. Accessed December 3, 2022.
2. Tsao CW, Aday AW, Almarzooq ZI, et al. Heart Disease and Stroke Statistics-2022 Update: A Report From the American Heart Association [published correction appears in Circulation. 2022 Sep 6;146(10):e141]. Circulation. 2022;145(8):e153-e639. doi:10.1161/CIR.0000000000001052
3. Centers for Disease Control and Prevention. Heart Disease Facts. https://www.cdc.gov/heartdisease/facts.htm. Published October 14, 2022. Accessed December 3, 2022.
4. McGee S. Chapter 39 Auscultation of the heart: General principles. ScienceDirect. https://reader.elsevier.com/reader/sd/pii/B9780323392761000391?token=4E9CEA029CF0C6A3BAC31EA75E3C24C46EB1D73631C716504BB94BDD60830B4351008C3CDCDE9EF97921C36EB1D5A016&originRegion=us-east-1&originCreation=20230324130835. Published 2018. Accessed March 24, 2023.
5. American Heart Association. How the Healthy Heart Works. www.heart.org. https://www.heart.org/en/health-topics/congenital-heart-defects/about-congenital-heart-defects/how-the-healthy-heart-works. Published March 24, 2022. Accessed December 3, 2022.

6. Anatomy of the Heart Image. Cardiology Associates of Michigan; 2019. https://www.cardofmich.com/anatomy-human-heart-fun-facts/. Accessed December 3, 2022.
7. Pollock JD, Makaryus AN. Physiology, Cardiac Cycle. [Updated 2022 Oct 3]. In: StatPearls [Internet]. Treasure Island (FL): StatPearls Publishing; 2022 Jan. Available from: https://www.ncbi.nlm.nih.gov/books/NBK459327/
8. Heart Conduction System (Cardiac Conduction). Cleveland Clinic. https://my.clevelandclinic.org/health/body/21648-heart-conduction-system. Published July 23, 2021. Accessed December 3, 2022.
9. Eisner DA, Caldwell JL, Kistamás K, Trafford AW. Calcium and Excitation-Contraction Coupling in the Heart. Circulation Research. 2017;121(2):181-195.doi:10.1161/CIRCRESAHA.117.310230
10. Schipperheyn JJ. The pathophysiology of potassium and magnesium disturbances. A cardiac perspective. Drugs. 1984;28 Suppl 1:112-119. doi:10.2165/00003495-198400281-00012
11. Anatomy and function of the heart's electrical system. Anatomy and Function of the Heart's Electrical System. https://www.hopkinsmedicine.org/health/conditions-and-diseases/anatomy-and-function-of-the-hearts-electrical-system. Published August 8, 2021. Accessed December 3, 2022.
12. Bernard Karnath M, William Thornton M. Auscultation of the Heart. Review of Clinical Signs. Turner White Communications, Inc.; 2002:39-43. https://docplayer.net/21007913-Auscultation-of-the-heart.html

13. Ismail S, Siddiqi I, Akram U. Localization and classification of heart beats in phonocardiography signals —a comprehensive review. EURASIP Journal on Advances in Signal Processing. 2018/04/27 2018;2018(1):26. doi:10.1186/s13634-018-0545-9
14. Arora N, Mishra B. Origins of ECG and Evolution of Automated DSP Techniques: A Review. IEEE Access. 2021;9:140853-140880. doi:10.1109/ACCESS.2021.3119630
15. Phanphaisarn W, Roeksabutr A, Wardkein P, Koseeyaporn J, Yupapin P. Heart detection and diagnosis based on ECG and EPCG relationships. Med Devices (Auckl). 2011;4:133-144. doi:10.2147/MDER.S23324
16. Dornbush S, Turnquest AE. Physiology, Heart Sounds. [Updated 2022 Jul 18]. In: StatPearls [Internet]. Treasure Island (FL): StatPearls Publishing; 2022 Jan. Available from: https://www.ncbi.nlm.nih.gov/books/NBK541010/
17. Kusko MC, Maselli K. Introduction to Cardiac Auscultation. In: Taylor AJ, ed. Learning Cardiac Auscultation: From Essentials to Expert Clinical Interpretation. Springer London; 2015:3-14.
18. Institute for Quality and Efficiency in Health Care (IQWiG). What Is an Electrocardiogram (ECG)?; 2019. Accessed December 4, 2022. https://www.ncbi.nlm.nih.gov/books/NBK536878/
19. Klabunde RE. Electrocardiogram standard limb leads (bipolar). Cardiovascular Physiology Concepts. https://www.cvphysiology.com/Arrhythmias/A013a. Published November 29, 2022. Accessed December 3, 2022.
20. Ashley EA, Niebauer J. Cardiology Explained. London: Remedica; 2004. Chapter 3, Conquering the ECG. Available from: https://www.ncbi.nlm.nih.gov/books/NBK2214/

21. Electrocardiogram. Mount Sinai Health System. https://www.mountsinai.org/health-library/tests/electrocardiogram. Accessed December 3, 2022.
22. Shafiq G, Tatinati S, Ang WT, Veluvolu KC. Automatic Identification of Systolic Time Intervals in Seismocardiogram. Nature. 2016; 6(1):37524. doi:10.1038/srep37524
23. Korzeniowska-Kubacka I, Kuśmierczyk B, Bilińska M, Dobraszkiewicz-Wasilewska B, Mazurek K, Piotrowicz R. Seismocardiography - A non-invasive method of assessing systolic and diastolic left ventricular function in ischaemic heart disease. Folia Cardiologica. 2006; 13:319-325.
24. Zanetti JM, Tavakolian K. Seismocardiography: Past, present and future. 2013: 7004-7007.
25. Rai D, Thakkar HK, Rajput SS, Santamaria J, Bhatt C, Roca F. A Comprehensive Review on Seismocardiogram: Current Advancements on Acquisition, Annotation, and Applications. Mathematics. 2021; 9(18):2243. https://doi.org/10.3390/math9182243
26. Taebi A, Solar BE, Bomar AJ, Sandler RH, Mansy HA. Recent Advances in Seismocardiography. Vibration. 2019; 2(1):64-86. https://doi.org/10.3390/vibration2010005
27. Voyatzoglou A. An Introduction to the Comparison of Seismocardiography and Phonocardiography. Honors Undergraduate Theses. 2022. Available from: https://stars.library.ucf.edu/honorstheses/1217.
28. Lubner RJ, Kondamuri NS, Knoll RM, et al. Review of Audiovestibular Symptoms Following Exposure to Acoustic and Electromagnetic Energy Outside Conventional Human Hearing. Front Neurol. 2020;11:234. Published 2020 Apr 28. doi:10.3389/fneur.2020.00234